IN VITRO CHARACTERIZATION AND NUCLEAR DELIVERY OF POLY(3-HYDROXYBUTYRIC ACID-CO-3-HYDROXYVALERIC ACID) (PHBV) BASED NANOPARTICLES

A THESIS SUBMITTED TO
THE GRADUATE SCHOOL OF NATURAL AND APPLIED SCIENCES
OF
MIDDLE EAST TECHNICAL UNIVERCITY

BY

AYLA ŞAHİN

IN PARTIAL FULFILLMENT OF THE REQUIREMENTS
FOR
THE DEGREE OF MASTER OF SCIENCE
IN
BIOTECHNOLOGY

SEPTEMBER 2015

Approval of the Thesis:

IN VITRO CHARACTERIZATION AND NUCLEAR DELIVERY OF POLY(3-HYDROXYBUTYRIC ACID-CO-3-HYDROXYVALERIC ACID) (PHBV) BASED NANOPARTICLES

submitted by **AYLA ŞAHİN** in partial fulfillment of the requirements for the degree of **Master of Science in Department of Biotechnology**, **Middle East Technical University** by,

Prof. Dr. Gülbin Dural Ünver
Dean, Graduate School of **Natural and Applied Sciences** _____

Prof. Dr. Filiz Bengü Dilek
Head of Department, **Biotechnology** _____

Prof. Dr. Vasıf Hasırcı
Supervisor, **Biological Sciences Dept., METU** _____

Prof. Dr. Nesrin Hasırcı
Co-Supervisor, **Chemistry Dept., METU** _____

Examining Committee Members:

Prof. Dr. Gamze Köse
Genetics and Bioengineering Dept., Yeditepe University _____

Prof. Dr. Vasıf Hasırcı
Biological Sciences Dept., METU _____

Assoc. Prof. Dr. Rengül Atalay
Informatics Institute, METU _____

Assoc. Prof. Dr. Sreeparna Banerjee
Biological Sciences Dept., METU _____

Assoc. Prof. Dr. Dilek Keskin
Engineering Sciences Dept., METU _____

Date: 09.09. 2015

I hereby declare that all information in this document has been obtained and presented in accordance with academic rules and ethical conduct. I also declare that, as required by these rules and conduct, I have fully cited and referenced all material and results that are not original to this work.

Name, Last Name: Ayla Şahin

Signature:

ABSTRACT

IN VITRO CHARACTERIZATION AND NUCLEAR DELIVERY OF POLY(3-HYDROXYBUTYRIC ACID-CO-3-HYDROXYVALERIC ACID) (PHBV) BASED NANOPARTICLES

Şahin, Ayla

M.S., Department of Biotechnology

Supervisor: Prof. Dr. Vasıf Hasırcı

Co-Supervisor: Prof. Dr. Nesrin Hasırcı

September 2015, 92 pages

The use of polymeric nanoparticles in life sciences as drug carrier vehicles has been expanding because of their ability to penetrate sites not accessible to larger particles and their large surface area-to-volume ratios that increase their drug release rates. The main objective of this study was to prepare nano sized polymeric particles to deliver active compounds across cell membranes and preferably into the nuclei. This would improve the biostability of macromolecular drugs (growth factors and polynucleotides), and increase their efficacy. Nanocapsules of poly(3-hydroxybutyric acid-co-3-hydroxyvaleric acid) (PHBV) were prepared to study their penetration into the nuclei of Saos-2 human osteosarcoma and L929 cells. The polypeptide based nuclear targeting agent, Nuclear Localization Signal (NLS), was used to improve localization and an anticancer agent, Doxorubicin, was used to study the effectiveness of the PHBV nanoparticles as drug carriers.

Keywords: Biodegradable Nanoparticles, Nuclear Drug Delivery, Drug Targeting, Doxorubicin, Nuclear Localization Signal.

ÖZ

POLİ(3-HİDROKSİBÜTİRİK ASİT-KO-3-HİDROKSİVALERİK ASİT) (PHBV) KÖKENLİ NANOPARÇACIKLARIN *İN VİTRO* KOŞULLARDA KARAKTERİZASYONU VE HÜCRE ÇEKİRDEĞİNE GÖNDERİLMESİ

Şahin, Ayla
Yüksek Lisans, Biyoteknoloji Bölümü
Tez Yöneticisi: Prof. Dr. Vasıf Hasırcı
Ortak Tez Yöneticisi: Prof. Dr. Nesrin Hasırcı
Eylül 2015, 92 sayfa

Polimerik parçacıklar, yüzey alanı-hacim oranı büyük olduklarından ve daha büyük parçacıkların içine giremediği alanlara girebilme özelliklerinden dolayı, yaşam bilimlerinde ilaç taşıyıcı araçlar olarak gün geçtikçe daha fazla kullanılmaktadırlar. Bu çalışmanın temel hedefi nano boyutta polimerik parçacıkları hazırlayarak, aktif bileşimleri hücre zarından ve tercihen hücre çekirdeğinden geçirmektir. Bu makromoleküler ilaçların (büyüme faktörleri ve polinükleotidler) biokararlılıklarını geliştirecek ve etkilerini artıracaktır. Poli(3-hidroksibütirik asit-ko-3-hidroksivalerik asit) kökenli PHBV nanokapsüller, Saos-2 insan osteosarkom ve L929 hücrelerinin çekirdek içlerine girmelerini çalışmak için hazırlanmıştır. Polipeptit kökenli çekirdeksel hedefli ajan, çekirdek lokalizasyon sinyali (ÇLS), lokalizasyonu geliştirmek ve Doxorubicin antikanser ajanı PHBV nanotaneciklerinin etkenliğini karşılaştırmak için kullanılmıştır.

Anahtar Kelimeler: Biyobozunur Nanoparçacıklar, Hücre Çekirdeğine İlaç Taşımı, İlaç Hedefleme, Doxorubicin, Hücre Lokalizasyon Sinyali

Dedicated to my family

ACKNOWLEDGEMENTS

I would like to express my most sincere gratitude to my supervisor Prof. Dr. Vasıf Hasırcı for his continuous guidance, advice, encouragement, support and insight throughout my thesis. I am grateful for his patience and effort to improve my scientific experience during my graduate years.

I am also grateful to my co-supervisor Prof. Dr. Nesrin Hasırcı for her support, guidance, useful comments and suggestions. I was fortunate for her mentoring which improved my scientific experience to an international level.

I would like to express my special thanks to Gözde Eke and Gökhan Bahçecioğlu for their patience, endless support, help and being there for me all the time I needed them throughout this thesis.

I wish to express my gratitude to Dr. Arda Büyüksungur for his encouragement, deep understanding and advices about my studies. I would like to thank him for his patience during CLSM analysis.

I would like to thank all the members of BIOMATEN-METU Center of Excellence in Biomaterials and Tissue Engineering and my labmates, Sepren Öncü, Cemile Kılıç, Ayşe Selcen Alagöz, Esen Sayın, Tuğba Dursun, Menekşe Ermiş Şen, Senem Heper, Deniz Sezlev Bilecen, Damla Arslantunalı, Aylin Kömez, Büşra Günay, Ezgi Antmen, Bilgenur Kandemir, Assoc. Prof. Dr. Erkan Türker Baran and our technician Zeynel Akın for their support in this study.

Finally, I would like to express my deepest gratitude to my precious family members who supported me in any respect during my life. I owe my deepest gratitude to my mother, Nilüfer Şahin, my father Osman Şahin, and my precious beloved brother Emre Şahin for their understanding, endless love, caring, support, patience and trust in me not only for this study, but for all my life.

TABLE OF CONTENTS

APPENDICES

LIST OF TABLES

TABLES

LIST OF FIGURES

FIGURES

LIST OF ABBREVIATIONS

BSA	Bovine Serum Albumin
CALCEIN	3, 3’-Bis [N,N-bis(carboxymethyl) aminomethyl] fluorescein
CLSM	Confocal Laser Scanning Microscopy
DAPI	4',6-diamidino-2-phenylindole
DIC	Differential Interference Contrast
DMEM	Dulbecco’s Modified Eagle Medium
DMSO	Dimethyl Sulfoxide
DNA	Deoxyribonucleic Acid
DOX	Doxorubicin
EDC	1-Ethyl-3-(3-dimethylaminopropyl)-carbodiimide
FBS	Fetal Bovine Serum
FITC	Fluorescein isothiocyanate
HA	Hyaluronic acid
NC	Nanocapsule
NHS	N-Hydroxysuccinimide
NLR	Nile Red
NLS	Nuclear Localization Signal
NPC	Nuclear Pore Complex
PTX	Paclitaxel
PBS	Phosphate Buffer Saline
PHBV	Poly(3-hydroxybutyric acid-co-3-hydroxyvaleric acid)
PVA	Polyvinylalcohol

CHAPTER 1

INTRODUCTION

1.1. Drug Delivery Systems

Drug administration is an important aspect of biotechnology and pharmacy which makes a significant impact on the effectiveness of bioactive agents. Various drug delivery vehicles including micro and nano particles have been developed and have shown the ability to carry a variety of therapeutic agents such as small molecules, peptides and protein-based drugs, and recently, nucleic acids for gene therapy purposes. These bioactive agents are introduced to micro and nano-carrier structures in order to modify the solubility and stability of drug molecules providing an opportunity for the drugs which were ignored earlier because of their poor pharmacokinetics when in free form. Micro and nano-sized carriers are a special and promising category of drug delivery because of their small size which helps them overcome biological barriers and penetrate the membranous barriers. The drug carriers used for medical purposes should be hemocompatible (not cause adverse reactions in the blood) and biocompatible (not cause adverse reactions throughout the body). If the carriers are made up of degradable molecules, their degradation products must also be biocompatible (Parveen et.al., 2012).

Drug delivery systems mask undesirable taste and odor of the drugs, decrease their systemic availability if targeted actively or passively, thus decrease systemic side effects, and prolong the availability. Besides, drug concentration in the target area is increased. Handling of the drug becomes easier.

During the design and preparation of delivery systems, the most important properties are dimension and form of the carrier, the drug loading method, the stability or

degradation properties of the carrier and the chemical compatibility of the drug and the carrier. Nanocarriers are able to be safely introduced intravenously (i.v.) and they can circulate in blood stream for long periods without the recognition by reticuloendothelial cells, so they have a longer time to reach their target and pass through the biological membranes including those of the cells (Hasirci, 2007, De Villiers et.al., 2009)

1.1.1. Carrier Materials

A variety of organic and inorganic materials are used in drug delivery. Organic materials can be of synthetic or natural origin and they are versatile because they can be chemically modified to change their properties. Some of the synthetic and all the biological materials are biodegradable, which is an advantage because this prevents them from accumulating in the body and lead to problems. Inorganic carriers such as hydroxyapatite (HAp) and zeolite are also used as carriers under certain conditions and mostly as composites formed with polymers as or 3D scaffold structures.

1.1.1.1. Natural Polymers

Natural origin polymers have various characteristics such as biocompatibility, biodegradability, water binding capacity and they can be modified or conjugated with other molecules by using certain chemical and enzymatic reactions. The enzymes that are found in biological systems can hydrolyze or degrade these polymers and metabolize their products. There are also certain disadvantages of these polymers. They can induce immune response, the sources of these polymers may have a batch-to-batch variability or could be limited. Examples for natural origin polymers can be bovine serum albumin (BSA), collagen, gelatin, hyaluronic acid, chitosan, polysaccharides (cellulose derivatives such as carboxymethyl cellulose).

Collagen is a structural protein and a major constituent of biological systems. It is non-toxic and biocompatible, and it can be resorbed in the body. Although it has a high cost and variability in properties depending on its source, it has superior

biocompatibility when compared with gelatin and albumin. It can also be used in combination with various natural and synthetic polymers (Zuber et al., 2015).

Gelatin has no antigenicity under physiological conditions which makes it convenient to use as a carrier material. A great advantage of using gelatin as a carrier material is that it has a low cost. Gelatin has been extensively used to deliver both hydrophilic and hydrophobic anti-cancer drugs such as doxorubicin, cisplatin and paclitaxel where they increased the efficiency of the controlled release and targeting of the mentioned drugs (Elzoghby, 2013).

Hyaluronic acid (HA) is mostly found in connective tissues of biological systems. It is biodegradable, non-immunogenic, non-toxic and has high water binding properties which makes them ideal as carrier materials (Xu et.al., 2006). The hyaluronic acid-drug conjugates are combined by using chemical linkers in order to overcome certain disadvantages of free drug molecules. For example, Paclitaxel (PTX), which is an anticancer drug, has poor solubility, toxic, side effects and drug-resistance in the body and the HA-PTX conjugates suppress the undesirable effects of PTX showing a strong toxicity towards certain cancer cell types (Zhang et.al., 2014). It has been reported that hyaluronic acid that was prepared as Doxorubicin carrying nanogels showed a significant antitumor effect on three different cell lines (Yang et al., 2015).

Chitosan is a non-toxic, biodegradable and low cost natural polymer which is also used in the formation of hydrogels. The acetylation level and molecular weight of chitosan can be varied in order to have various mechanical and hydrophilic properties (Elgadir et al., 2014). It was reported that Paclitaxel loaded chitosan nanoparticles has shown induced macrophage uptake of three different cancer cell lines (Prabaharan, 2015).

1.1.1.2. Synthetic Polymers

Synthetic polymers also have appropriate characteristics for use as carrier materials. Most biodegradable synthetic polymers are biocompatible and does not cause any immunological responses when they are compared with some of natural origin ones. They can be altered to have different mechanical properties or degradation rates and their properties can also be modified to enhance their roles. Among the most important carriers are synthetic polymers such as acrylates which have a number of pH responsive examples such as Eudragit. Silicones have also been an important category which has been used in birth control. Poly(vinyl alcohol) (PVA) has also been used as a surfactant in the development of carrier systems.

PLA, PGA and their copolymer PLGA are the most commonly used synthetic polymers as carrier materials because of their biodegradability and biocompatibility. They have acidic degradation products which are lactic acid and glycolic acid, so they are suitable for responsive release systems (Makadia et.al., 2011, Crucho et.al., 2015). Misra et.al (2010) stated that Doxorubicin loaded PLGA nanoparticles had increased antiproliferative effect the cytotoxicity on MCF-7 cells compared with free Doxorubicin drug.

PEG is used as a chemical enhancer at low concentrations (Park et al., 2009). Addition of PEG to nanoparticle surface enhances the circulation time of the carrier since it inhibits nonspecific protein adsorption which leads to opsonization and clearance of the carrier from the biological system (Park et al., 2009). Zhang et al. (2014) stated that PEG-PLGA micelles had a great potential in tumor-targeting since PEG increased the stability of the carrier and prolonged its circulation time.

1.1.1.3. Polyhydroxyalkanoates (PHAs)

PHAs are most commonly used polymers in drug delivery. They are mostly produced by bacteria (Urtuvia et.al., 2014) and transgenic plants (Yilgor et.al., 2008, Ciesielski et.al., 2014). Table 1 shows the types of PHAs that are produced by microorganisms (Gürsel and Hasirci, 1995).

Table 1: Different types of PHAs produced by microorganisms (Gürsel & Hasirci, 1995)

Monomer	**R-Group**	**Polymer**
β -hydroxybutyrate (HB)	CH_3 (methyl)	PHB
β -hydroxyvalerate (HV)	CH_2CH_3 (ethyl)	PHV
β -hydroxycaproate (HC)	$CH_2CH_2CH_3$ (n-propyl)	PHC
β -hydroxyheptanoate (HH)	$CH_2(CH_2)_2CH_3$ (n-butyl)	PHH
β -hydroxyoctanoate (HO)	$CH_2(CH_2)_3CH_3$ (n-pentyl)	PHO
β -hydroxynonanoate (HN)	$CH_2(CH_2)_4CH_3$ (n-hexyl)	PHN

They are linear, bioresorbable, biodegradable and biocompatible (Chen et.al., 2014, Leong et.al., 2014). The mechanical properties, crystallinity and degradability of PHAs are determined by their composition and molecular weight. PHAs are slowly hydrolyzed in human body; however, by changing the composition, the rate of hydrolysis can be regulated. This allows the changing of the degradation time of the polymer according to the desired applications (Pouton et.al., 1996) (Figure 1 A) Some PHA formulations such as poly(3-hydroxybutyrate) (P3HB) and its copolymers with 3-hydroxyvalerate, poly(3-hydroxybutyrate-co-3-hydroxyvalerate) (PHBV) has been commonly used in the controlled release systems for the delivery of certain drugs such as anticancer agents, growth factors or antibiotics (Chen et.al., 2005, Yilgor et.al., 2008) (Figure 1 B).

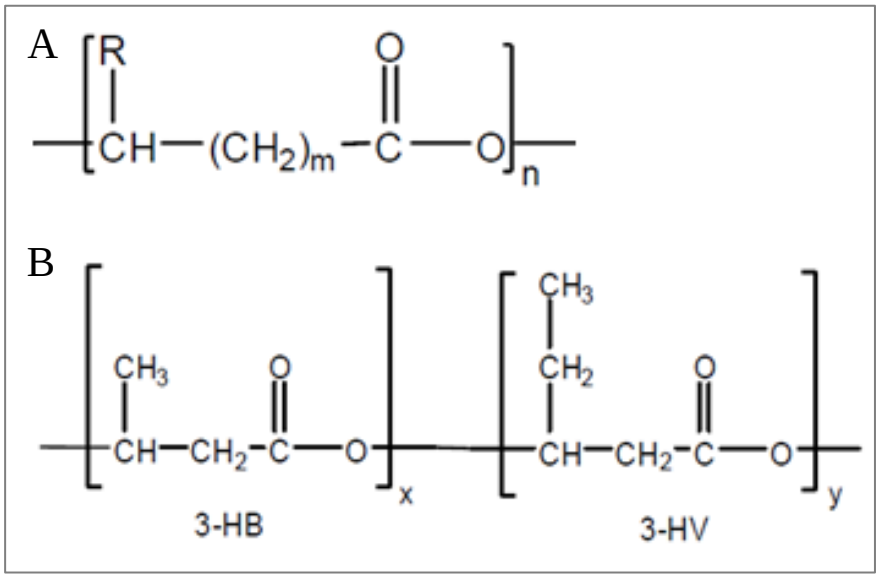

Figure 1: Molecular structure of polyhydroxyalkanoates and a copolymer poly(3-hydroxybutyrate-co-3-hydroxyvalerate). A) Polyhydroxyalkanoate general formula. When m=1 and R=CH_2CH_3, the product is poly(3-hydroxyvalerate) (PHV). B) Poly(3-hydroxybutyrate-co-3-hydroxyvalerate) (PHBV). x and y can be in the range of several thousands.

1.1.2. Lipid-Based Drug Delivery Systems

1.1.2.1. Liposomes

Liposomes are defined as spherical lipid vesicles that are composed of amphiphilic phospholipids with a bilayer membrane structure having a central aqueous void which forms a closed bilayer structure. The hydrophobic tails of the phospholipid membrane structure are protected from the aqueous environment by forming a bilayer structure whereas the hydrophilic head groups face the aqueous environment on the inside and outside (Parveen et al., 2012, Safinya et.al., 2012) (Figure 2).

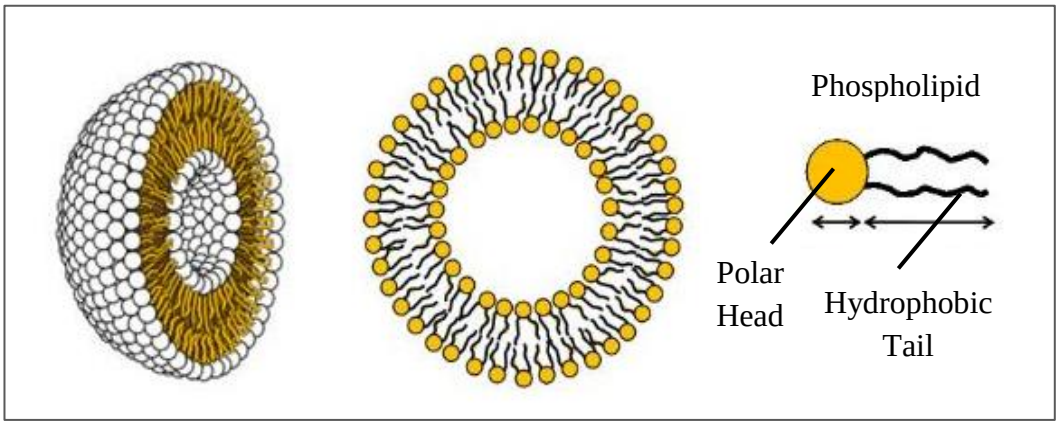

Figure 2: Schematic illustration of liposomes (Adapted from Bitounis et.al., 2012).

Liposomes firstly attracted researchers due to its structure that is similar to biological membranes where the lipid composition can form a model system. In 1965, the first publication was described by Alex Bangham and colleagues at the Agricultural Research Council Institue of Animal Physiology at Abraham (Düzgüneş & Gregoriadis, 2005) who established the basis of liposomal structure for model membrane systems where they suggested that phospholipids can form closed bilayer structures in an aqueous system (Bangham et.al., 1967). These researchers suggested various enclosed phospholipid bilayer structures such as the one that is formed by single bilayers called as "bangosomes" and later they were able to make single bilayer liposomes. Within a few years, there were many published papers related with the application of liposomes in different approaches. Sessa and Weissman were the first ones to discover the potential of these structures in their usefulness as carriers and they suggested the encapsulation of lysozyme in multilamellar vesicles (MLVs) (Sessa & Weissmann, 1968). By this time, with the recognition of the biodegradability, biocompatibility, low toxicity, immunogenicity and the ability of liposomes to entrap various molecules, Gregory Gregoriadis published four papers during the period from 1971 to 1976 as a pioneer to show that liposomes can change in vivo distribution of drugs that are entrapped in their structure and they can be used as carriers of drug delivery systems (Gregoriadis, 1973, Gregoriadis, 1976, Yang et al., 2011). Later, two more papers were published on the large unilamellar liposomes (LUVs) that are prepared with improved novel methods to trap the drug molecules in

a more efficient and homogenous way in their structure (Szoka & Papahadjopoulos, 1978). Since liposomes do not remain in circulation in sufficient time, long circulating liposomes were developed by coating their surface with inert and biocompatible polymers called as polyethyleneglycol (PEG) (Papahadjopoulos et al., 1991).

The liposome size ranges from 20 nm to 10 μm and can consist of single or multiple bilayers; small unilamellar vesicles (SUV), large unilamellar vesicles (LUV) and multilamellar vesicles (MLV) (Figure 3). Entrapment of both hydrophilic and hydrophobic pharmaceutical agents, in the core or in the membrane, respectively, is possible. Their size, charge and surface properties can be modified by using appropriate lipoid molecules during the preparation phase. One major disadvantage is their instability, and therefore, destruction before they can complete their task as drug delivery vesicles (Kim, 2007, Akbarzadeh et al., 2013). Liposomes are PEGylated in order to extend their systemic circulation which promotes their tumor uptake via EPR effect (see section 1.2.2.) and reduces free drug concentration in plasma (Kaminskas et al., 2012).

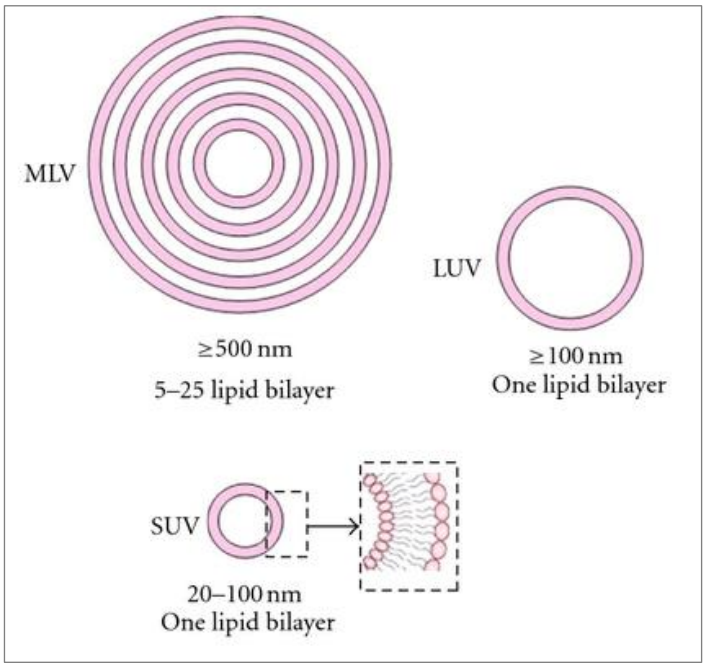

Figure 3: Various types of liposomes (Feng et. al., 2011).

1.1.2.2. Solid - Lipid Nanoparticles (SLNs)

Solid lipid nanoparticles (diameter range 50 nm – 1 μm) are composed of a solid matrix at room and body temperature. They are incorporated with the drug molecule and stabilized by certain surfactants (Figure 4). They can be constructed from highly purified trigylcerides, complex glyceride mixtures or even waxes. SLNs are an alternative to polymeric nanoparticles which are identical to oil-in-water emulsion. SLNs have many advantages in drug delivery such as high biocompatibility, biodegradability, stability, controlled release and enhanced drug efficacy due to their low toxicity. These are the advantageous features of the liposomes, fat emulsions and polymeric nanoparticles. However, unlike other tools, SLN solid matrix does not allow hydrophobic drug leakage making it resistant against release of drug during the storage. In addition, they have low drug loading capacities (Orive et.al., 2004, Prow et al., 2011, Pradhan et.al., 2013).

1.1.2.3. Micro/Nanoemulsions

Microemulsions (diameter range 1 - 1000 μm) or nanoemulsions (diameter range 5 nm - 1 μm) are transparent systems of two phases that are composed of two immiscible liquids (oil and water) mixed and stabilized by an interfacial surfactant film or mixture of surfactants (Figure 4). The advantages of these systems are the spontaneous formation, thermodynamic stability, simple production, high surface area-to-volume ratio. They can carry hydrophobic and hydrophilic drugs in the same emulsion system. The major disadvantage of these systems is their limited solubilizing capacity for high-melting substances since their stability is influenced by temperature and pH which affects the delivery of the drug inside the body (Sosnik et. al., 2010, Fanun, 2012, Pradhan et al., 2013).

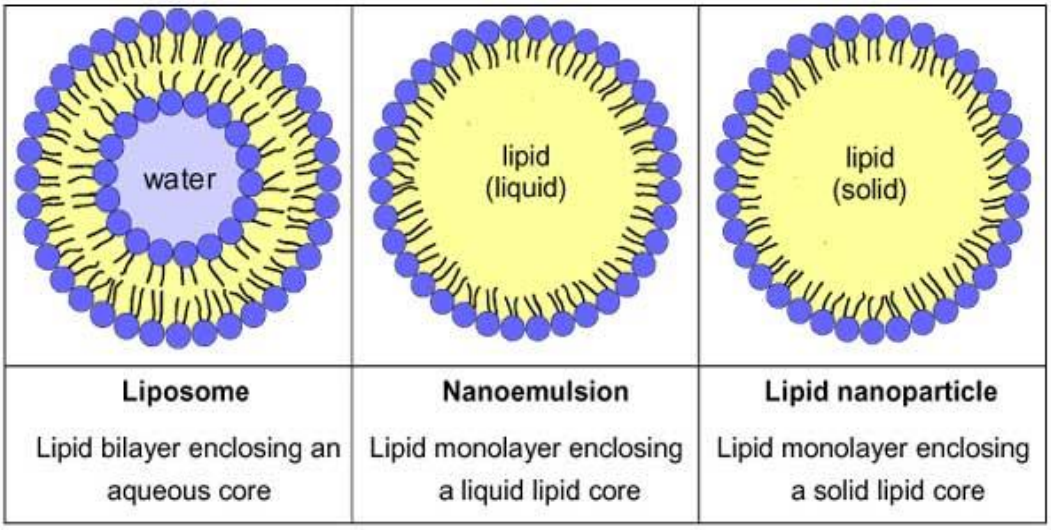

Figure 4: The structure of nano-sized lipid structures (Uchechi et.al., 2014).

1.1.3. Polymer-Based Drug Delivery Systems

1.1.3.1. Dendrimers

Dendrimers are defined as synthetic, tree-like structures that are formed by symmetrical macromolecular compounds around an inner core where the size (diameter range 1.5 - 10 nm) and shape can be altered as desired (Figure 5). They are polymeric molecules that are composed of multiple, perfectly branched chains that come out of a central core. Due to their highly branched structure, conjugating dendrimers with different ligands such as hydrophobic and hydrophilic drugs or with targeting moieties provide us a suitable targetable drug delivery vehicle. Dendrimers can be made by various polymers such as polyamidoamines (PAMAMs), polyamines, polyamides, polyesters, carbohydrates and DNA (Sosnik et al., 2010, Pradhan et al., 2013).

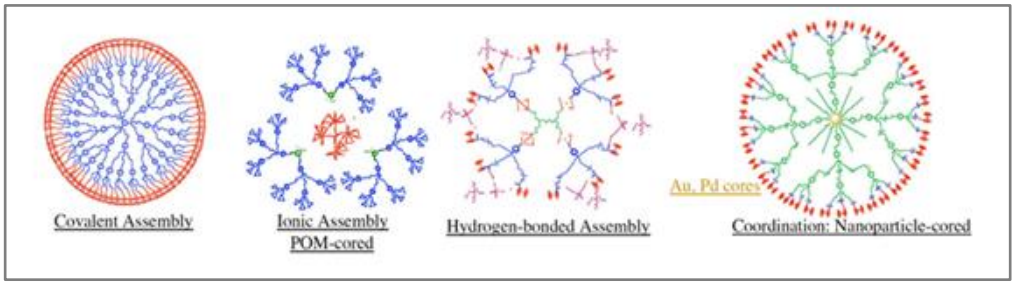

Figure 5: Different types of dendrimers (Adapted from Safari et.al, 2014).

1.1.3.2. Micelles

Micelles (diameter range 3 – 50 nm) are self assembled amphiphilic molecules that are similar to liposomes except that they exhibit a higher ordered structure consisting of monolayers while liposomes are made up of lipid bilayers. Standard micellar structures are formed at very high concentrations in the aqueous medium with a hydrophobic core surrounded by a hydrophilic shell. Micelles minimize toxicity and side effects of certain drugs, have high drug loading capacity, suitable controlled release profile and good biocompatibility (Figure 6) (Parveen et al., 2012, Kompella et. al., 2013).

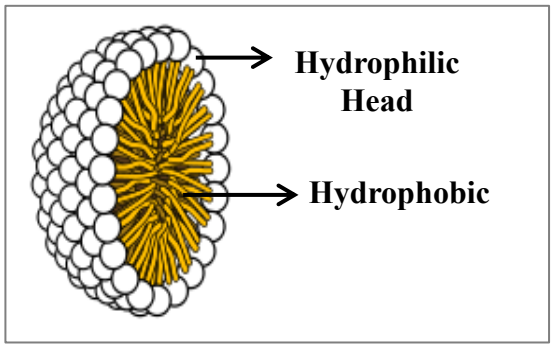

Figure 6: Schematic representation of a micelle composed of single lipid layer. (Adapted from Bitounis et.al., 2012).

1.1.3.2.1. Polymeric Micelles

Polymeric micelles are formed by block copolymers that have both hydrophilic and hydrophobic units that self assemble and form a hydrophobic core stabilized by a hydrophilic shell in an aqueous environment (Figure 7). Due to their very small sizes

(20-100 nm) polymeric micelles can leave the blood vessels and accumulate in tumor tissue (Gupta et.al., 2015). Recently, many drug loaded polymeric micelles were used for anticancer preclinical studies in order to improve the toxicity of cancer drugs in tumor cells. For instance, PEG-micelle formulations of a doxorubicin loaded polymeric micelle passed phase 1 clinical trials for solid tumors (Plapied et.al., 2011; Vilar et.al., 2012, Lu et.al., 2013). Torchilin et.al. (2013) states that the antitumor antibody-conjugated polymeric micelles called immunomicelles that encapsulate a water insoluble drug Taxol can recognize and bind to various cancer cells effectively *in vitro*.

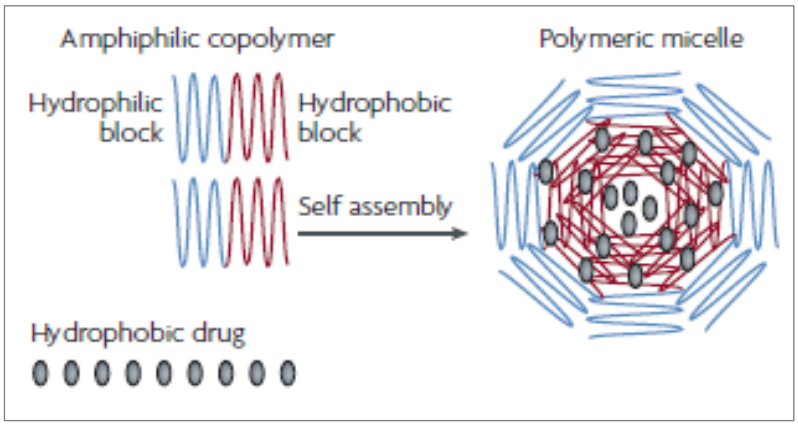

Figure 7: Assembly of a polymeric micelle (Torchilin et.al., 2013).

1.1.3.3. Hydrogels

Hydrogels are hydrophilic polymeric networks which have the ability to absorb large quantities of water and remain insoluble in aqueous solutions due to the chemical or physical crosslinking of individual polymer chains. Some hydrogels have the ability of transition in response to various physical and chemical stimuli such as temperature, electric or magnetic field, light, pressure, pH, solvent composition and ionic strength of the medium. In order to control the drug release behavior with physiological conditions, the hydrogel drug delivery system must sense the changes in the local environment and alter its drug release profile. Most of the time, the drug release occurs upon swelling of the hydrogel (Pradhan et al., 2013).

1.1.3.4. Micro/Nanospheres

Microspheres (diameter range; 1 μm – 1 mm) or nanospheres (diameter range; 10 nm- 1 μm) can be constructed of polymeric molecules (Figure 8).

It is possible to produce various fabrication types of spherical particles tailored to targeting of tissues, high specificity and highly controlled release. Release from these particles may occur with a burst release, diffusion through pores or with polymer erosion. The type of release in spherical particles is affected by the properties of the polymer and the drug loaded, particle size and the preparation techniques. A polymeric micro/nanosphere has a matrix type solid core. In this matrix structure, drug molecules can be entrapped, adsorbed or chemically bound to the polymeric chains. The drug molecules are generally entrapped in a dispersed form throughout the polymer matrix so that the drug molecule is both located on the surface and inside the spherical structure (Wang et.al., 2012).

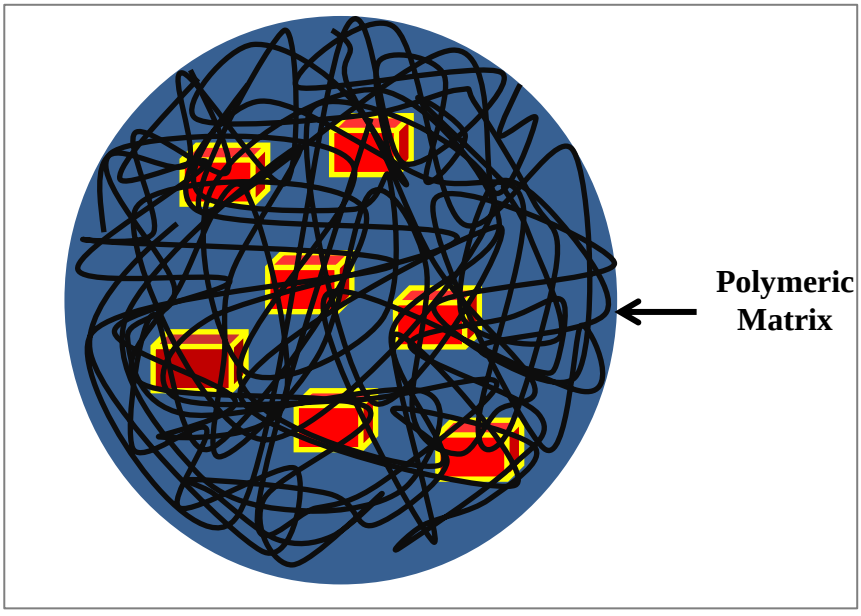

Figure 8: Micro and nanospheres. Drug crystals (red) are distributed through the polymeric matrix.

1.1.3.5. Micro/ Nanocapsules

Micro/nanocapsules are often considered reservoir systems since they have a core that generally contains the loaded active drug and is separated from the environment via a polymeric membrane which controls the rate of permeation of the contents and the solvent outside (Wang et.al., 2012) (Figure 9).

The active agent in the core can diffuse through the membrane at a constant release rate if the concentration gradient between the inside and the outside can be preserved which makes these systems suitable for Zero Order drug delivery applications (Elaissari et.al., 2010). The capsule cavity may contain the active agent in liquid or solid form or as a dispersion. However, the nanocapsule may also be made to carry the active agent on its surface or in embedded form in the membrane layer. There are six classical methods that can be used in the preparation of micro/nanocapsules: nanoprecipitation, emulsion-diffusion, double emulsification, emulsion-coacervation, polymer coating and layer-by-layer coating (Steichen et al., 2013, Torchilin et.al., 2013, Safari et. al., 2014).

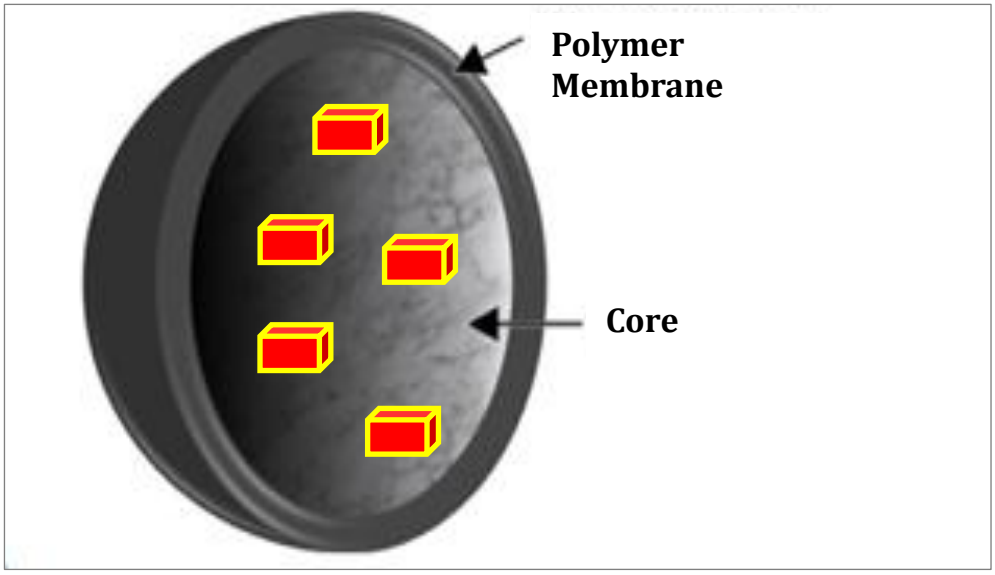

Figure 9: Schematic illustration of micro/nanocapsules. In this example the drug crystals (red) are located in the core.

1.1.4. Other Carriers

1.1.4.1. Quantum Dots

Quantum dots (QDs) are composed of 10-50 atoms of inorganic compounds such as Cd and Zn and their diameter range from 2 to 10 nm (Biju et.al., 2010). When they are exposed to UV, they tend to fluoresce in different colors depending on their size and their inorganic constituents. While the larger particles emit the red light, smaller particles tend to emit the blue light. Thus, they have a broad absorption and narrow emission characteristics making them suitable for cellular imaging (Probst et.al., 2013). Their main function is not to carry drugs but rather show where they are. A major challenge in using QDs for drug delivery is that they are generally toxic and must be coated with a polymeric layer. Coating of quantum dots with short chain peptides helps the penetration of these particles into cancer cells and this increases their success rate in drug delivery (Nie et.al., 2007, Probst et. al., 2013)

1.1.4.2. Carbon Nanotubes

Carbon nanotubes (CNTs) are carbon cylinders composed of benzene rings. They are cylindrical structures that are composed of single (the single walled, SWNTs) or multiple (multi walled, MWNTs) concentric graphene sheets (Figure 10). In contrast to other nanomaterials, CNTs are more dynamic in their biological application due to their nano needle shape and hollow monolithic structure so that these materials can enter the cell by various methods such as passive diffusion across the lipid bilayer or by directly endocytosis where the nanotubes attach to cell surface and engulfed inside the cell via the cell membrane (Choudhary et.al., 2001, Xu et al., 2006). CNTs can be used in the delivery of anticancer drugs. It has been reported that CNT-DOX drug delivery systems were based on the covalent linkage of DOX onto CNT by using an enzymatic reaction and this system demonstrated an efficient delivery of DOX in melanoma cancer cells (Wong et al., 2013).

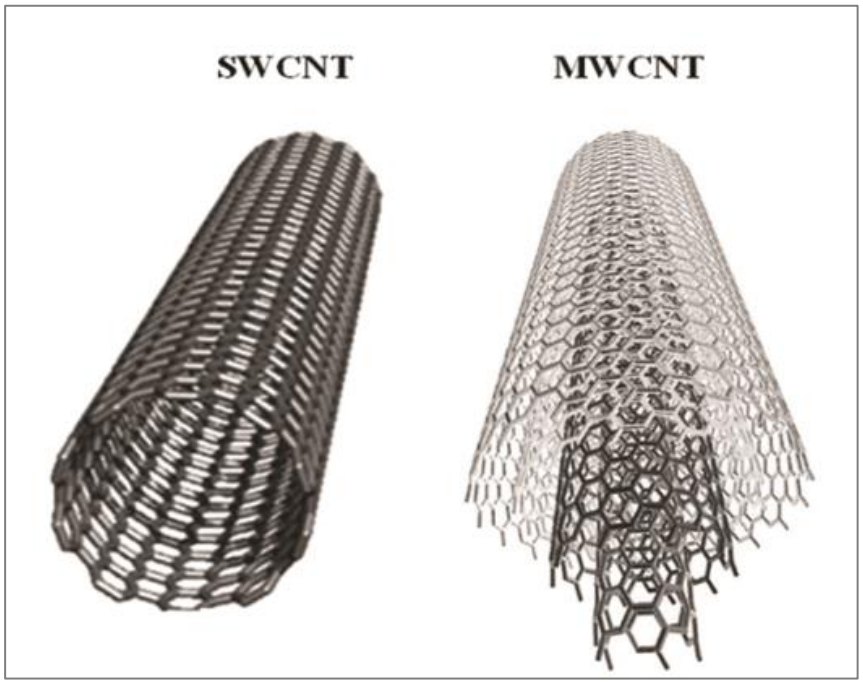

Figure 10: The single-walled (SWNTs) and multi-walled (MWNTs) (Choudhary et.al., 2001).

1.2. Controlled Release of Drugs

Drug delivery systems are generally designed to provide the drug level in the blood to be maintained in a therapeutic range which is the region between the Miniumum Effective Concentration (MEC) and the Minimum Toxic Level (MTL) (Figure 6). When a dose is administered, the drug level in the plasma is increased with a First order kinetics and then, it is eliminated also with the First order kinetics, leading to a gradual decline in the plasma level of the drug. To complete the therapy, the drug has to be administered several times and this creates a saw tooth appearance. Because of the frequent need for application and sometimes pain (if the drug is administered through i.v. route), this leads to poor patient compliance. Another risk is toxicity when drug is applied at high doses. Such systems provide sustained or prolonged release but not constant rate release. Certain drug carrier systems were developed in order to provide a controlled release without a need for frequent administration (Park, 2014, Lee et. al., 2015) (Figure 11).

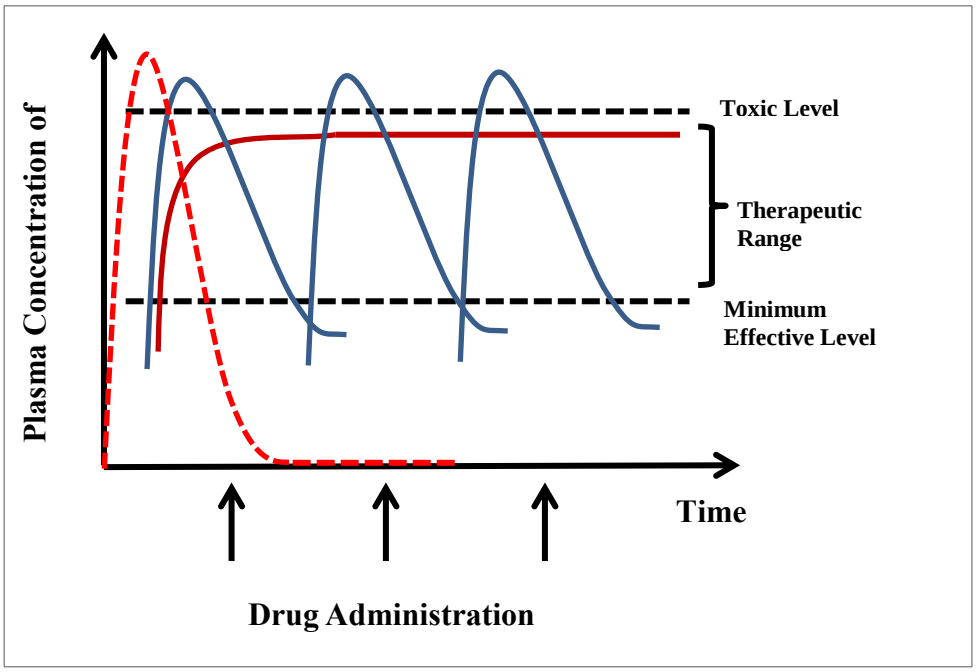

Figure 11: Drug concentration in plasma after administration. Single dose (red dashed line), multiple dose (blue line) (1st Order Kinetics) and Zero Order release (red solid line).

1.2.1. Release Kinetics in Drug Delivery

Drug release from carrier systems depends on several parameters which include the drug load, detention of the release systems, the ratio of drug and polymer, physical or chemical interactions between the carrier and the drug and the method used in the production of the carrier system.

Drug release may occur in different ways (Figure 12).

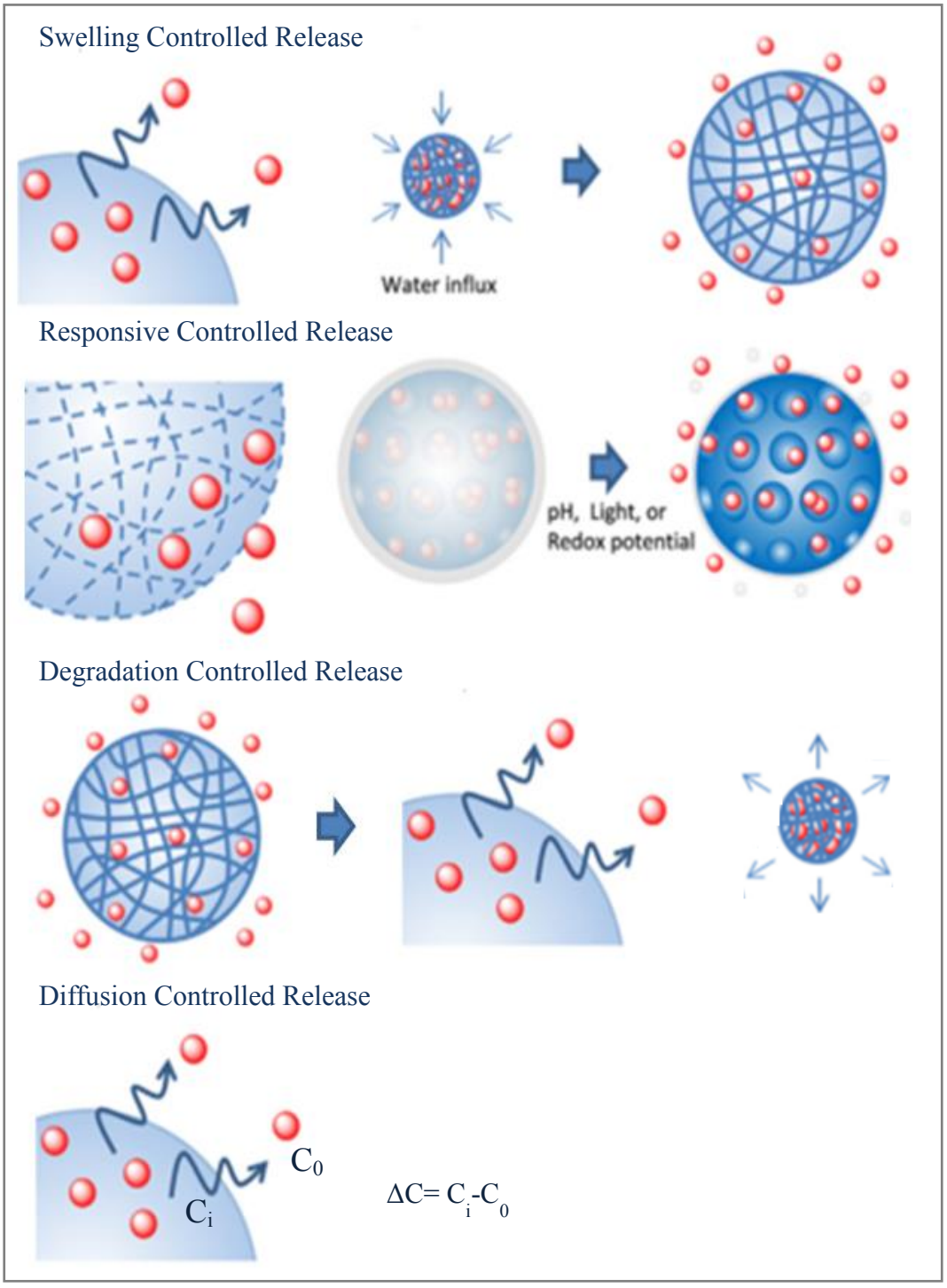

Figure 12: Different drug release types (Adapted from Lee et. al., 2015).

1.2.1.1. Diffusion Controlled Release

In this case, the drug leaves the particle by diffusion through the polymeric membrane of a reservoir (capsule) system or polymeric matrix of a sphere.

In the case of reservoir systems, the drug molecules are generally located in the core and are surrounded by a rate controlling membrane. Thus, the rate of release depends on the surface area, the membrane thickness, the interaction between the matrix and the drug concentration gradient between the system and outside. If the concentration gradient remains constant (the drug must create a saturated system), the release rate does not change with time and a zero order controlled release is obtained.

In the case of matrix systems, however, the drug molecules are dispersed within the polymeric matrix. Firstly, the drug molecules at or close to the surface are released. This causes the drug molecules in the matrix to gradually migrate to the surface to be released which takes a longer time (Park, 2014, Lee et. al., 2015). The release rate decreases with time and sometimes in proportion to the square root of time, which is called Higuchi release model (Higuchi, 1961). This equation $M_t/M_\infty = k.t^{1/2}$ is generally valid up to release of 40% of the drug content, where M_t is the amount of drug released at a time (h), M_∞ is the amount of drug released at time infinity (h), t is time (h) and k is the rate constant.

1.2.1.2. Degradation (Resorption) Controlled Release

This type of release is controlled by the rate of resorption of the carrier material of the system. In this process, the carrier gradually resorbs either through dissolution or degradation (simple or enzymatic hydrolysis) and releases the drug bound, entrapped or surrounded by the system (Aulton et.al., 2013). The rate of release is controlled by the rate of hydration of the carrier, the solubiliy of the drug in the medium, the thickness of the membrane (if it is a reservoir system) and the size of the carrier. If the surface-to-volume ratio of a spherical system (small size) is higher, this leads to a higher rate of release (Wise, 2000, Hillery et.al., 2003, Siepmann, et.al., 2011).

1.2.1.3. Swelling Controlled Release

Swelling controlled release systems are mostly based on crosslinked hydrophilic polymers or partially hydrophilic polymers. When the polymer is in dry state, polymer network is dense and the macromolecules do not have mobility. Upon the contact of polymer with water, the macromolecules gain mobility and the volume of the system increases but this has a limit because the crosslinks control the extent of swelling. This change leads to high penetration of medium and also increase in the distance between the polymer chains. This initiates the release process. If the system is constructed of a partially hydrophilic polymer, then the chains do not completely lose contact due to limited polymer and medium interaction. Thus, release is initiated by the medium imbibed. By changing the physical state of the polymer between nonswollen and swollen, the release rate of the drug can be controlled. In nonswollen state, the drug that is incorporated into polymer network is not mobile and effectively entrapped. Upon the contact with aqueous fluids, the water that diffuses into the system causes the relaxation of polymer chains. Then, the drug dissolves and diffuses through this swollen polymeric network. Drug diffuses out according to the concentration gradient between the swollen system and the outside (Hillery et.al., 2003, Siepmann et al., 2011, Tsung et.al., 2012, Lee et. al., 2015).

1.2.1.4. Responsive Controlled Release

In this case, the drug release is triggered by causing changes of certain factors in the external environment such as temperature, pH, ionic strength, ultrasound, electric or magnetic fields. For example, in the case of thermoresponsive drug carriers, the change in the medium temperature results in the phase transition of the polymer and induces it to extend or contract. In another example, the difference in pH of intracellular and extracellular environment can lead to swelling or shrinking of the carrier and be used to trigger the release of drug in different pH tissue compartments (lysosomes, cancer tissue, stomach, intestines) or different local temperature that might be achieved externally (Park, 2014, Lee et.al., 2015).

1.2.2. Targeted Drug Delivery

Although the controlled release systems can determine the rate of drug release, they are not able to control the fate or the distribution of drug inside the body. Therefore, targeted delivery systems are introduced to achieve site-specific or targeted drug delivery. In conventional drug administrations, once the drug enters the body, it is distributed throughout the body controlled by the barriers to be crossed and this wide distribution may take the drug to sites where their effect is detrimental and may result in undesirable side effects. Drugs are metabolized mainly in the liver and eliminated by the excretion through the kidneys, intestines and skin. In a systemic administration, only a fraction of the drug can reach to the intended tissue where the disease or the defect resides. At the targeted tissue, the drug can be rapidly cleared by metabolism or diffusion and may not be available long enough at a satisfactory concentration to perform its desired effect. The drug may be too hydrophilic, too large, too fragile or cannot be transported effectively by active, facilitated or passive transport due to its chemistry or other properties. In order to overcome these limitations, targeting systems must be designed. Such systems can protect the drug from being metabolized and its transport to the correct cells at high concentrations may be facilitated (Hillery et al., 2003, Lee et.al., 2015). Targeted drug delivery improves the distribution and the amount of the drug at the specific cells or tissues. The main component of a targeted delivery system is the targeting agent or moiety which carries the drug to the appropriate site or has a specific interaction capability with the target. There are certain requirements for effective drug targeting: the targeting system must be non-toxic, the drug should be able to reach the target site in active or prodrug form and the delivery and release of the drug should be at the target site. The targeting mechanisms can be divided into two main types: passive and active (Figure 13).

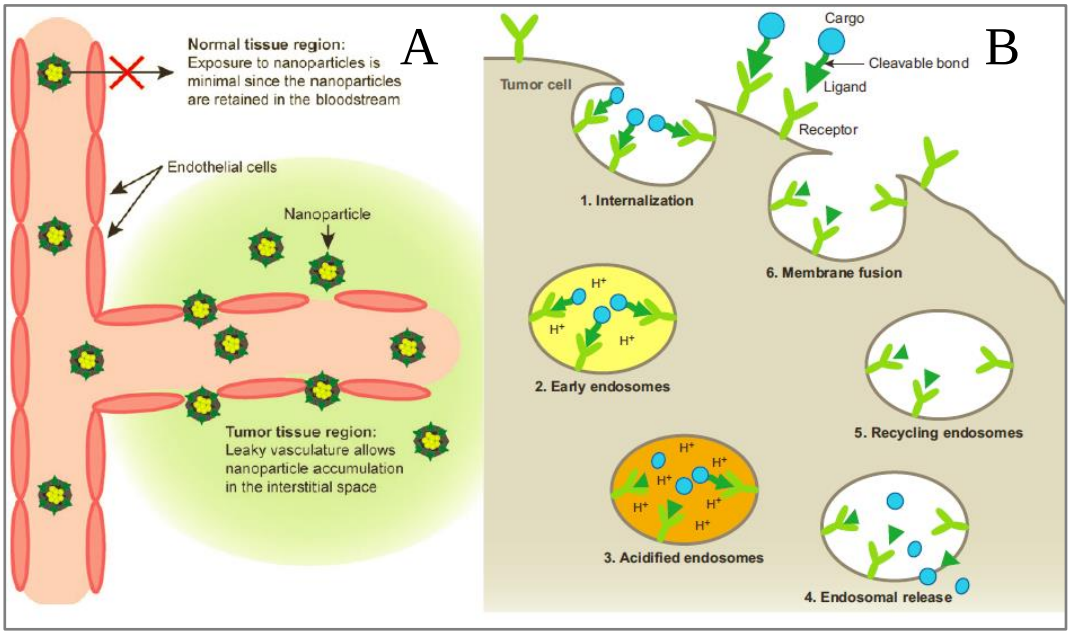

Figure 13: Drug Targeting. A) passive, and B) active (Yu et.al., 2013).

A common passive targeting system is called Enhanced Permeation and Retention (EPR) which benefits from the increased endothelial fenestrations of the vascular system (200-300 nm) at the hard tumor sites (Parhi et.al., 2012, Biswas et.al., 2013, Bertrand et.al., 2014). Thus, when the drug carrier of a certain size (< 50 nm) is administrated intravenously (i.v.), then the particles carrying the drug extravagate at the site where the tumor is.

Active targeting relies on the interaction between the targeting agent that is attached to the drug or the surface of the carrier and the target cell or tissue (Pouton et.al., 2007, Minko et.al., 2013). Thus, it is important for the targeting moiety to interact with the molecules or receptors at the target site in order to achieve the transport of the drug. The agents may target certain receptors to bind to the cell membrane or to facilitate the endocytosis of the drug or the carrier by the cell (Figure 14) (Hofmann et al., 2011). The carrier may bind to the surface and release its drug through the cell membrane or it can be endocytosed in the intact form by fusing with endosomal vesicle. Then, either the vesicle fuses with lysosomal vesicle which leads to the enzymatic degradation of the carrier or the carrier escapes from endosomal vesicle

and release its content into the cytoplasm (Figure 14 A). The carrier can also be recognized by the cell through a specific moiety on its surface, which will initiate its uptake. This targeting moiety can be an antigen that is normally recognized by the antibodies in plasma. These specific antibodies induce the targeting of the carrier through antigen binding (Figure 14 B). For example, certain viral envelope proteins can be conjugated on the carrier. These protein structures have been reported to have antitumorigenic applications in preclinical and clinical trials and also approved for use as influenza vaccine (Glück et.al., 1999; Marchisio et al., 2002), against malaria (Okitsu et al., 2007, Cech et al., 2011), HIV (Bomsel et al., 2011) and viral bronchiolitis (Kamphuis et al., 2012).

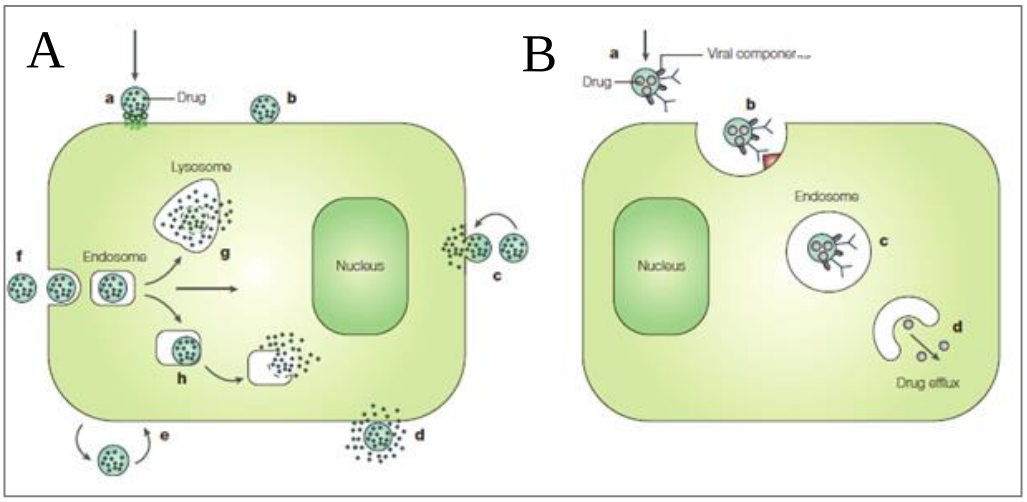

Figure 14: The route of a targeted carrier upon binding to the cell membrane (Hofmann et al., 2011).

The drug may also be bound to magnetic compounds and the drug can be concentrated in the target area by using magnetic fields (Pouton et.al., 2007, Perrie et.al., 2012). The targeting moiety can be either tumor-specific or tissue specific. Tumor-specific moieties are generally ligands that recognize the upregulated receptors on tumor tissue, so by identifying receptors on specific tumor types, the carriers can be targeted actively. Certain galactose derivatives (Heath et.al., 2008, Deng et.al., 2012) and transferrin (Cui et.al., 2013) are examples to these type of ligands.

1.2.2.1. Targeted Delivery to the Cell Nucleus

Mammalian cells are highly compartmentalized and membrane-bound compartments. Thus, upon the entry of the drug molecules into the cytosol, they are quickly distributed among the compartments according to the property of the drug and intracellular environment. The nucleus is separated from the rest of cytoplasm by the double membrane structure of the nuclear envelope which constitutes a major barrier and the main rate limiting step in the transport of drug into the nucleus. The envelope contains nuclear pore complexes (NPCs) that allow certain molecules to diffuse freely or through a facilitated or an energy-dependent transport mechanism. The NPCs form channels that allow the transport of small polar molecules, ions and macromolecules such as proteins and RNAs between the cytoplasm and the nucleus. They are composed of three domains: a central domain, a nuclear and cytoplasmic ring (Pouton et al., 2007). The central and nuclear domains are anchored to the ring moiety and to each other by filaments that protrude toward the cytoplasm and extend into the nucleus (Figure 15).

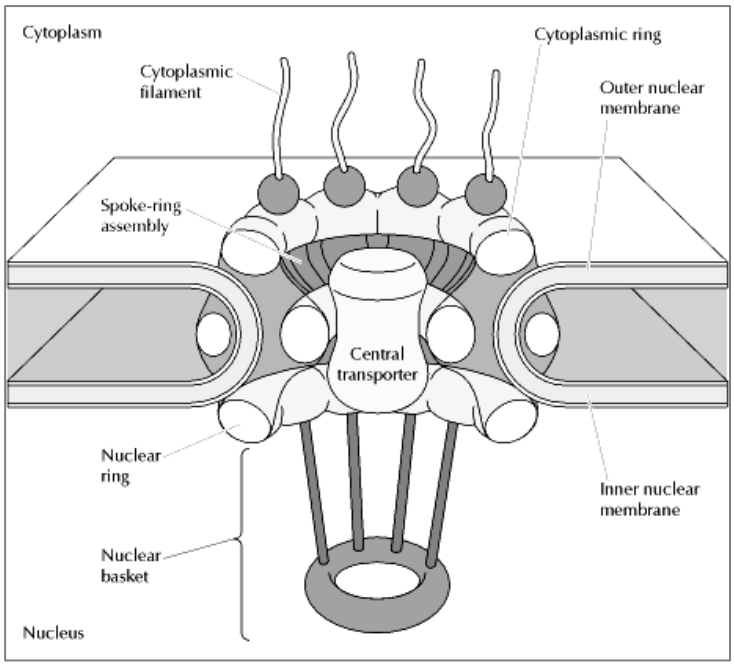

Figure 15: The Nuclear Pore Complex (NPC) (Pouton et al., 2007).

The NPC has a diameter of 120 nm and is composed of 50-100 different proteins. The small molecules or proteins with molecular mass smaller than 50 kD can passively diffuse through these channels (about 9 nm in diameter). However, proteins and RNAs are selectively transported via an active transport mechanism. The active transport through nuclear pores is achieved by the specific amino acid sequences called nuclear localization signals (NLS) that mediate the shuttling between the cytosol and the nucleus. Lys-Arg and Lys-Lys sequences are required for nuclear targeting where the sequences other than these are ineffective in nuclear localization. The transport of certain molecules through nuclear pores is mediated through some homologous proteins called importins and exportins. The import mechanism can be divided into two steps (Figure 16). In the first step, the molecule that contains NLS binds to the nuclear pore complex through importin; this step does not require energy. NLS consists of two subunits: importin α and importin β. Importin α binds to NLS and importin β binds to the cytoplasmic filaments which brings the target molecule to the nuclear pore. The second step involves an energy-dependent process where importin α is transported through the nuclear pore into the nucleus together with its cargo, releasing importin β to the cytosol and importin α to the nucleus. In this energy-dependent process, Ran protein, which is a Ras-like protein that has a GTP binding cassette, controls the GTP hydrolysis rate. Upon the binding of NLS containing cargo to the importin β, RanGTP is hydrolyzed into RanGDP When RanGTP is hydrolyzed into RanGDP. This results in a higher concentration of RanGDP in the cytoplasm. RanGDP is converted into RanGTP in the nucleoplasm since the enzyme that catalyzes this process is found in the nucleus resulting in a higher ratio of RanGTP/ RanGDP inside. Thus, the concentration gradient of these two protein complex drives the trafficking back and forth through the nuclear pore complex (Dean et. al., 2003, Belting et. al., 2005, Pouton et. al., 2007).

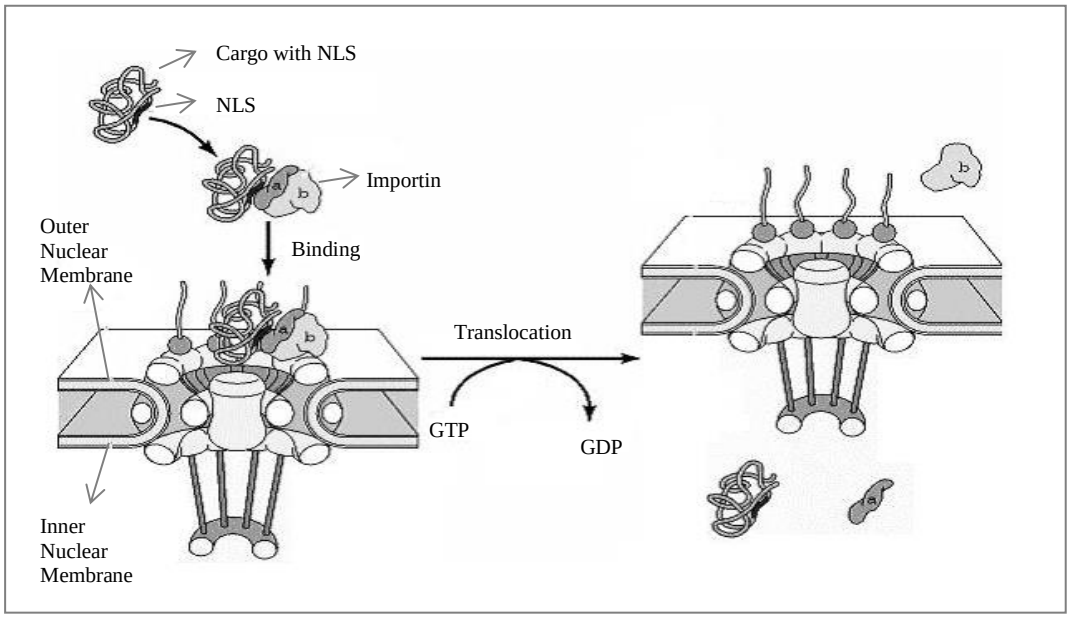

Figure 16: Nuclear transport. Upon the binding of cargo to the importin α through NLS, importin β binds to cytoplasmic filaments to target the carrier to the nuclear pore. The carrier is translocated through the nuclear pore with the energy-dependent process (GTP hydrolysis into GDP) (Pouton et al., 2007).

1.2.2.1.1. Barriers of Drug Delivery to the Nucleus

In order for the carrier to pass through the plasma membrane, it has to bind to the cell surface. Nanocarriers must be taken up via different uptake mechanisms due to their large sizes (Figure 17). Uptake may occur through either phagocytosis by phagocytes (macrophages, neutrophils and dendritic cells) or pinocytosis by all mammalian cell types. Endocytosis is the key step for intracellular and nuclear delivery of nanocarriers. After the internalization of nanocarriers into endocytotic vesicles (endosomes), they can be routed to lysosomes where they can be degraded inside the endo/lysosomal vesicle. This is a barrier to nuclear delivery of the drug molecules. At this step, the nanocarriers must be able to escape or disrupt the endo/lysosomal membrane to be released into the cytosol. Once inside the cytoplasm, the drug should show its biological activity on its molecular target. After this step, the nanocarriers approach the nuclear pore complex must be recognized by the NPC proteins which will help the entry of nanocarriers inside the nucleus. This recognition occurs

through the binding of NPC proteins to the nanocarriers that contain NLS molecules on their surfaces as is explained in section 1.2.2.1. (Sui et.al., 2011, Li et.al., 2012).

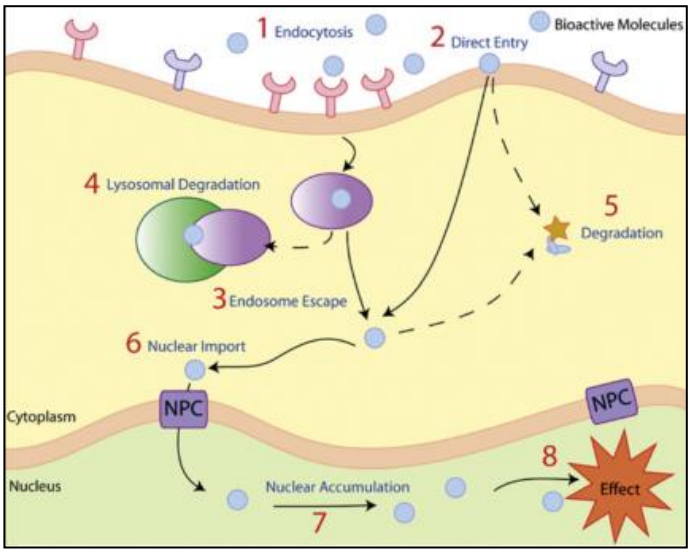

Figure 17: Barriers to drug delivery into the nucleus. (1) Nanocarrier should pass through the first barrier (plasma membrane) by endocytosis, (2) certain molecules such as certain proteins can enter directly. (3) Nanocarrier has to avoid degradation by avoiding the degradative enzymes (4, 5). (6) Nanocarrier must go through the final barrier by forming the NPC complex, in order to enter, and (7) accumulate in nucleus (8) in order to show its biological effect (Sui et al., 2011).

1.3. Bioactive Agents in Cancer Therapy

There are many types of anticancer agents that differ in their chemical structure and the mechanism of action on cancer cells. They mostly focus on damaging DNA in order to prevent cell cycle of cancer cells. The most commonly used anticancer agents belong to certain groups. Alkylating agents (Nitrogen mustards, Nitrosoureas) directly damage DNA and each can act on different phases of the cell cycle. Antimetabolites (Methorexate, 5-fluorouracil) interferes the S phase of cell cycle in order to interfere DNA or RNA growth. Anthracyclines (Doxorubicin, Epirubicin) blocks the enzymes that are involved in DNA replication (Nie et al., 2007).

1.3.1. Doxorubicin

Doxorubicin is a widely used drug in cancer treatment and has shown activity against both the solid and liquid tumors. Doxorubicin has an anthracycline structure and is isolated from a soil bacterium, *Streptomyces peucetius*. In general, anthracycline drugs prefer to intercalate between the DNA base pair that is connected to sugar moieties from one side which locate in the DNA minor groove (Figure 18).

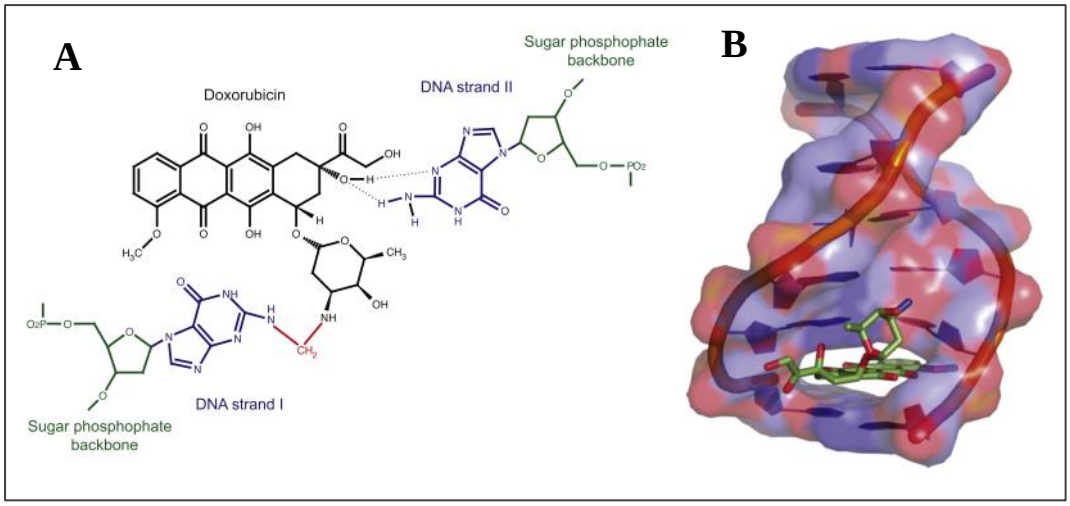

Figure 18: The mechanism of action of Doxorubicin. A) Doxorubicin forming a covalent bond (red) with the one strand of base pair and a hydrogen bond with the opposing strand, B) The intercalation of Doxorubicin with DNA, pushing the base pairs away from the sugar moiety that sits on minor groove (Yang et. al., 2014).

There are several models that have been proposed for its action on cancer cell death such as topoisomerase II poisoning (Pommier et.al., 2010), DNA adduct formation (Swift et.al., 2006), oxidative stress (Fan Yang et al., 2014) and ceramide overproduction. Topoisomerase II poisoning is the most commonly reported mechanism. In this model, the two types of topoisomerase enzymes, topoisomerase IIα and topoisomerase IIβ, are involved. During the replication and transcription, topoisomerase II binds to the DNA supercoil and this leads to the breakage in the strand of the DNA duplex and then, resealing of the break during DNA replication

and transcription. However, Doxorubicin traps topoisomerase II at the breakage site and prevents the resealing of the DNA (Tacar et. al., 2013, Yang et al., 2014)

1.3.2. Cisplatin

Cisplatin is a potent antitumor agent and is active against a variety of tumors (Figure 19). It is a hydrophilic drug and shows its action by interacting with DNA and form DNA adducts which activate certain signaling pathways that result in the apoptosis of the cancer cell (Tchounwou et.al., 2014). Adduct formation causes changes in DNA conformation that prevents DNA replication. Cisplatin can be inhibited by numerous mechanisms that result in drug resistance. In order to minimize this, combinational therapy of Cisplatin with other anticancer agents such as Doxorubicin were developed (Florea et.al., 2011).

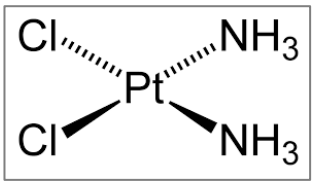

Figure 19: The chemical structure of Cisplatin.

1.3.3. Paclitaxel

Paclitaxel is a natural chemotherapeutic agent synthesized by the bacteria, *Taxus baccata.* It is commonly used against breast and ovarian cancer (Figure 20).

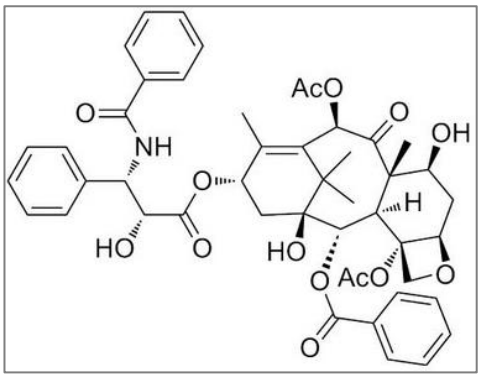

Figure 20: The chemical structure of Paclitaxel.

The drug shows its effect on microtubule organization by disrupting it to cause mitotic arrest which results in cell death through apoptosis (Choron et al., 2015). During the formation of microtubules, α and β tubulin proteins form a heterodimer structure which shows the distinct structural differences of both subunits. Microtubule formation is a dynamic structure where the tubulin dimers (α and β) undergo rapid assembly and disassembly (Krebs et.al., 2005) (Figure 21). Paclitaxel enhances the polymerization of tubulins which stabilizes them against depolymerization by its unique specific binding on the microtubules (Orr et.al., 2003).

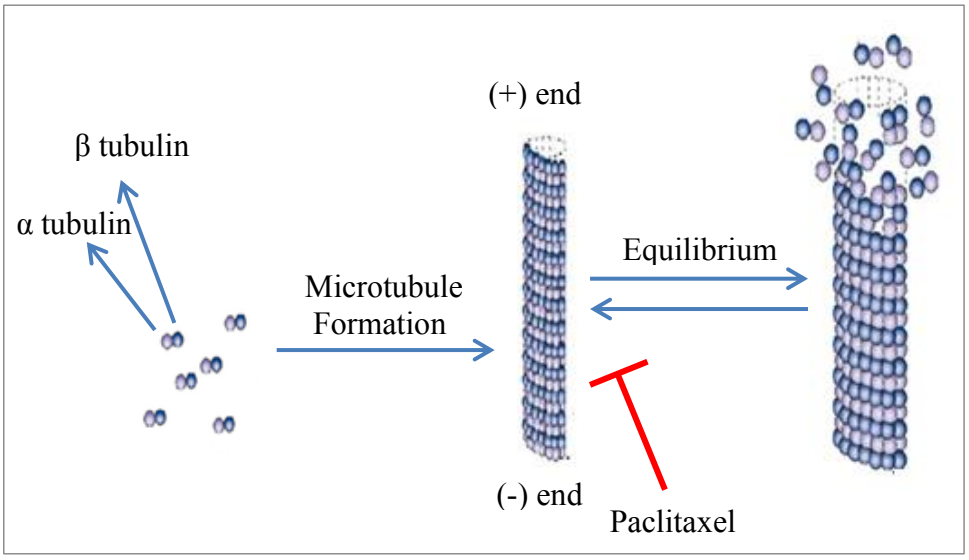

Figure 21: Mechanism of Paclitaxel action.

1.4. Aim and Novelty of the Study

The aim of this study was to develop a novel generation of polymeric nanoparticles to target the anti-cancer drug, Doxorubicin, to the cell nucleus. Doxorubicin blocks the cell replication by intercalating the DNA base pairs. Thus, Doxorubicin shows its effect directly on the cell DNA indicating that the drug must be efficiently delivered into the nucleus. In accordance with this, PHBV nanoparticles were selected as the drug carrier system. PHBV is a biodegradable, natural and nontoxic polymer, which is a suitable choice for drug delivery. Nuclear localization signal (NLS) was used as a targeting moiety to deliver the particles to the target and was covalently attached onto PHBV nanoparticle surfaces. PHBV nanoparticles were used for the first time in this study for a nuclear delivery application. Target cell used was the human osteosarcoma cell line, Saos-2. Since Saos-2 cells are of a bone cancer cell line and Doxorubicin is commonly used for bone cancer treatment, this pair of drug and cell type is a proper choice in studying the cytotoxic effect of Doxorubicin drug in a carrier mediated and targeted fashion. In order to generate a proper anti-cancer drug delivery system and understand the behavior of the system *in vitro*, two different populations of nanoparticles were prepared; one was Nile Red loaded PHBV nanocapsules where Nile Red was used as a fluorescent dye in order to determine the location of cell nuclei targeted nanoparticles *in vitro* and the other was Doxorubicin loaded PHBV nanocapsules where Doxorubicin was the anti-cancer drug. It was observed that the PHBV nanoparticles can penetrate into Saos-2 cells, accumulate near or on the nucleus and would potentially increase the cytotoxic effect of Doxorubicin in *in vivo* applications.

CHAPTER 2

MATERIALS AND METHODS

2.1. Materials

PHBV (HV content 11% molar), Doxorubicin hydrochloride (98.0-102.0%, HPLC), Calcein (3, 3'-Bis [N,N-bis(carboxymethyl) aminomethyl] fluorescein), N-Hydroxysuccinimide (NHS), chloroform, paraformaldehyde (37%), FITC-labeled Phalloidin, Alexa Fluor 488 Phalloidin and Draq 5 were purchased from Sigma-Aldrich (USA). NLS (DRQIKIWFQNRRMKWKK) peptide and EDC (1-Ethyl-3-(3-dimethylaminopropyl)-carbodiimide) were purchased from Thermo Scientific (USA). Polyvinyl alcohol (PVA, MW $1.5.10^4$) was from Fluka (USA). Alamar blue® was purchased from Invitrogen Inc. (USA). Human osteosarcoma cells (Saos-2) was purchased from the American Type Culture Collection (No: CCL-1, ATCC). RPMI-1640 medium, fetal bovine serum (FBS) and penicillin/streptomycin were obtained from HyClone (USA).

2.2. Methods

2.2.1. Nanoparticle Preparation

2.2.1.1. Preparation of Doxorubicin Loaded PHBV Nanocapsules

Nanocapsules encapsulating Doxorubicin (λ_{ex}: 480 nm, λ_{em}: 590 nm) were prepared by water-in-oil-in-water emulsion technique. Briefly, PHBV (60 mg) was dissolved in chloroform (0.6 mL, 10% w/v) to create a polymer solution. Doxorubicin was dissolved in ultrapure water (1 mg/ mL) and added into the polymer solution. This mixture was added into an aqueous solution of PVA (2 mL, 4% w/v) to create an

emulsion and sonicated for 30 s in an ice bath. Then, this emulsion was added into another PVA solution (0.3% w/v, 50 mL). Chloroform was evaporated by vigorous stirring with a magnetic stirrer at room temperature overnight. Nanocapsules were collected by centrifugation (18,000 rpm, 20 min), washed with distilled water, frozen at -20^{o}C and lyophilized (Figure 22).

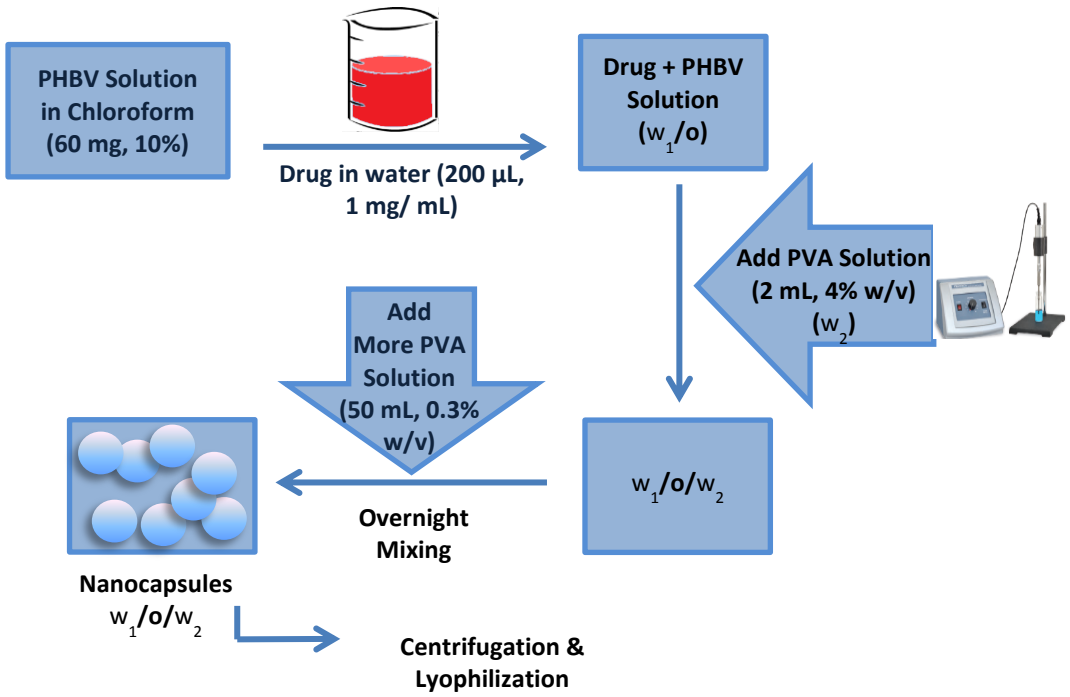

Figure 22: Preparation of Doxorubicin loaded PHBV nanocapsules by water-in-oil-in-water ($w_1/o/w_2$) emulsion technique.

During the optimization of the preparation of nanoparticles, the nanoparticle suspensions were centrifuged at different speeds (16000-18000 rpm) and durations (10-30 min). They were also exposed to different durations of sonication (15-30 s) in order to obtain the smallest particles. Thus, the procedure above includes the conditions to be able to prepare the particles with smallest sizes by changing two parameters explained above.

2.2.1.2. Preparation of Nile Red Loaded PHBV Nanocapsules

Loading of Nile Red (λ_{ex}:485 nm, λ_{em}:525 nm) in PHBV nanocapsules was carried out as described in section 2.1.1.1. where Doxorubicin was entrapped. The only difference is the use of dichloromethane instead of chloroform for dissolving the PHBV.

2.2.1.3. NLS Conjugation on PHBV Nanocapsules

The PHBV nanocapsules (10 mg) were suspended in ultrapure water (6 mL). EDC solution (300 μL, 1mg/ mL) in ultrapure water and NHS (300 μL, 1mg/ mL) in ultrapure water were added onto the suspended PHBV nanocapsules, consequently. The final solution was stirred with a magnetic stirrer for 1 h at 37^{o}C. The suspension was centrifuged (18,000 rpm, 20 min). After the centrifugation, the supernatant was removed. The pellet consisting of surface activated PHBV nanocapsules was suspended in 2 mL ultrapure water.

For the conjugation of NLS onto the PHBV nanocapsules, NLS (200 μL, 1 mg/ mL) in ultrapure water was added onto the surface activated PHBV nanocapsule solution and incubated for 1 h at room temperature. The final solution was frozen at -20^{o}C overnight and lyophilized for 6 h (Figure 23).

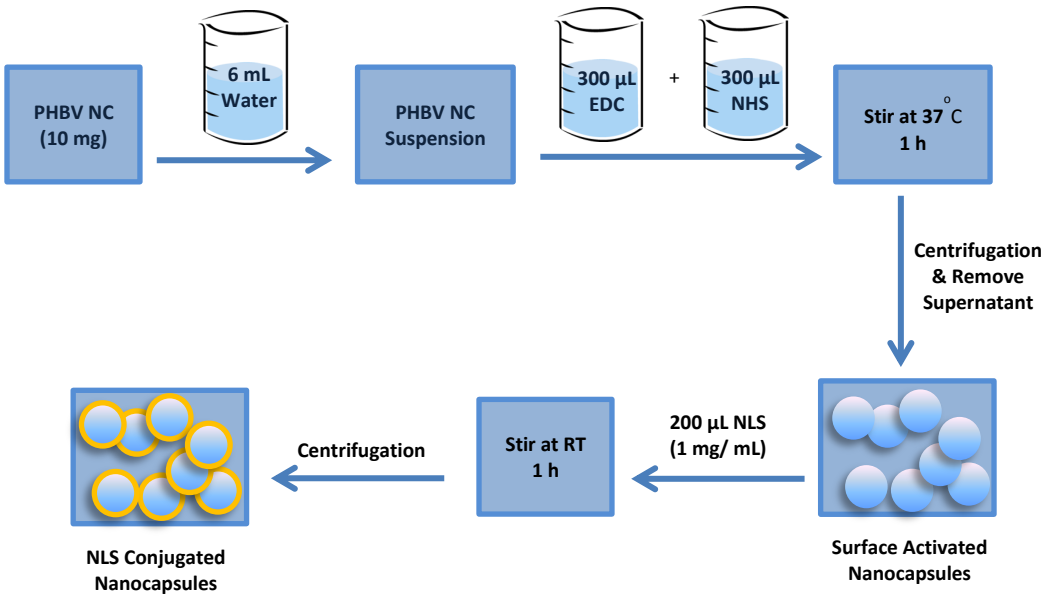

Figure 23: NLS conjugation on PHBV nanocapsules by EDC/NHS crosslinking.

2.2.2. Characterization

2.2.2.1. Morphology of PHBV Nanocapsules

PHBV nanocapsules were studied with scanning electron microscopy (QUANTA 400F Field Emission SEM, Netherlands). Nanocapsule suspension was added onto the carbon tapes attached to SEM stubs and coated with gold by using a sputter coater. The mean diameter of the nanocapsules was measured from the SEM micrographs using the Image J (NIH, USA) software.

2.2.2.2. Size Distribution of PHBV Nanocapsules

Determination of size distribution of PHBV nanocapsules was carried out using a Malvern Zetasizer (Nano ZS90, UK).

2.2.2.3. X-ray Photoelectron Spectroscopy (XPS) Analysis

XPS measurements were performed using the XPS-PHI (PHI 5000 VersaProbe, USA) instrument that uses a monochromatic Al X-ray source. For each sample, a survey scan was obtained and especially the regions belonging to N (390-410 eV)

and C (280-305 eV) were examined. The conjugation of NLS onto PHBV nanocapsules was shown using the C and N contents of the samples.

2.2.2.4. Doxorubicin Loading and Encapsulation Efficiency

Encapsulation efficiency (EE) is the fraction of the drug entrapped in a carrier system to the total drug added to the system at the beginning. The percent of EE is calculated according to the following equation:

$$\text{Encapsulation Efficiency (\%)} = \frac{\text{the amount of drug in the drug carrier system (mg)}}{\text{the amount of input drug (mg)}} \text{x}100 \quad \ldots\ldots\ldots \text{(I)}$$

Drug loading is the amount of the drug in unit drug containing carrier and is calculated according to the following equation:

$$\text{Drug loading (\%)} = \frac{\text{the amount of drug in drug carrier system (mg)}}{\text{the weight of carrier system containing drug (mg)}} \text{x}100 \quad \ldots\ldots\ldots\ldots\ldots\ldots \text{(II)}$$

The total amount of Doxorubicin in PHBV nanocapsules was measured with spectrofluorometer (Molecular Devices, SpectraMax M2, USA). Doxorubicin containing PHBV nanocapsules (20 mg) were dissolved in chloroform (3 mL), the absorbance values (λ_{ex}: 480 nm, λ_{em}: 590 nm) were recorded and the amount was calculated according to the calibration curve constructed by preparing known concentrations of Doxorubicin in water and recording the absorbance values using the same procedure (Appendix A).

2.2.2.5. Calcein Loading and Entrapment Efficiency

The concentration of Calcein in PHBV nanocapsules were measured with UV spectrophotometer (Molecular Devices, SpectraMax M2, USA). Calcein containing PHBV nanocapsules (20 mg) were dissolved in chloroform (3 mL), the absorbance values (λ_{ex}: 494 nm, λ_{em}: 517 nm) were recorded and the amount was calculated according to the calibration curve constructed by preparing known concentrations of Doxorubicin in water and recording the absorbance values using the same procedure (Appendix B).

2.2.2.6. *In situ* Doxorubicin Release From Nanoparticles

In the release studies, nanoparticles were suspended in ultrapure water (3 mL, 20 mg/mL) and placed in adialysis tubing (Snake skin, cut off MW 10,000 pleated, Thermo Scientific, USA). The tubings were placed in ultrapure water (10 mL). This medium was stirred on a magnetic stirrer at 37^{o}C for 35 days. At various time points (1h – 35 days), Doxorubicin released was measured at (λ_{ex} 480 nm, and λ_{em} 590 nm) by using a spectrofluorometer by taking samples from the medium. The measured samples were added back to the medium. The final data was plotted as released Doxorubicin concentration versus time and treated according to Higuchi Equation.

2.2.3. *In vitro* Studies

2.2.3.1. Determination of Saos-2 Cell Viability with Alamar Blue Cell Proliferation Assay

Alamar Blue cell proliferation assay was used to determine the number of live cells as it was done in earlier studies (Bahcecioglu et.al., 2014). This assay involves the spectrophotometric measurement of color change in sample which happens due to the reduction of Alamar Blue by the activity of mitochondrial enzymes. The extent of color change within the given duration is directly related with the cell number (Appendix C)

Osteosarcoma cells (human osteosarcoma cell line, Saos-2, Passage no: 8) were used for the *in vitro studies.* 24-well plates were seeded with Saos-2 cells ($2x10^4$ cells/ well). After incubation for 3 h, the medium was added onto the cells and the absorbance of the cells was measured at various time points. For each time point, medium was removed and the well was washed twice with sterile phosphate buffer saline (PBS) (10 mM, pH 7.4) and incubated for 1 h in Alamar Blue solution (1 mL, 1% penicillin/streptomycin, 10% Alamar Blue solution, 89% colorless DMEM high modified medium) in a CO_2 incubator (Sanyo MCO-17AIC, Japan). After incubation, 200 µL of this solution was transferred to a 96-well plate. The absorbance of the solution was measured at 570 nm (λ_1) and 595 nm (λ_2) by using Elisa Plate Reader

(Molecular Devices, USA). The reduction percent of Alamar Blue was calculated by using the following equation:

$$\text{Reduction (\%)} = \frac{[(\varepsilon_{ox})_{\lambda 2} \cdot A_{\lambda 1}] - [(\varepsilon_{ox})_{\lambda 1} \cdot A_{\lambda 2}]}{[(\varepsilon_{red})_{\lambda 1} \cdot A'_{\lambda 2}] - [(\varepsilon_{red})_{\lambda 2} \cdot A'_{\lambda 1}]} \times 100 \quad \text{..... (III)}$$

where,

$A_{\lambda 1}$: Absorbance of the sample at λ_1

$A_{\lambda 2}$: Absorbance of the sample at λ_2

$A'_{\lambda 1}$: Absorbance of negative control well (blank) at λ_1= 570 nm

$A'_{\lambda 2}$: Absorbance of negative control well (blank) at λ_2= 595 nm

ε_{ox}: Molar extinction coefficient of oxidized Alamar Blue

ε_{red}: Molar extinction coefficient of reduced Alamar Blue

$(\varepsilon_{ox})_{\lambda 1}$: 80.586

$(\varepsilon_{ox})_{\lambda 2}$: 117.216

$(\varepsilon_{red})_{\lambda 1}$: 155.677

$(\varepsilon_{red})_{\lambda 2}$: 14.652

The absorbances were converted to Reduction (%) and then to Cell Number using the calibration curve constructed using the same procedure with known number of cells (Appendix D).

2.2.3.2. Effect of Free Doxorubicin on Saos-2 Cell Viability (Dose-Response Study)

The effect of different concentrations of free Doxorubicin on Saos-2 cell viability was studied using the Alamar Blue Cell Proliferation Assay as explained in section 2.2.3.1. except that after attachment, some of medium was replaced with free Doxorubicin solution to achieve the final concentrations of 0.01, 0.10, 0.50, 1.0, 5.0, 10.0 and 100.00 μg/mL. The control group had only cells. The cell numbers were determined on Day 4 as explained above.

All the experiments were conducted in triplicate and the cell-free medium was used as the blank.

2.2.3.3. Effect of Doxorubicin Loaded PHBV Nanocapsules on Saos-2 Cell Viability

The effect of different concentrations of PHBV nanocapsules carrying Doxorubicin on the viability of Saos-2 cells was studied by Alamar Blue Cell Proliferation Assay. The test was carried out as in section 2.2.3.1. except that cell seeding density was 25,000/ well and after attachment, the medium was replaced with nanoparticles (1 mg/ mL) suspended in the culture medium. There were 4 groups of nanoparticles; (1) PHBV nanoparticles, (2) PHBV nanoparticles conjugated with NLS, (3) PHBV nanoparticles loaded with Doxorubicin and (4) PHBV nanoparticles loaded with Doxorubicin and conjugated with NLS (Table 2). The control group had only Saos-2 cells. The dye reduction (%) was measured on Day 4.

All the experiments were conducted in triplicate and the cell-free medium was used as the blank.

Table 2: The groups of nanoparticles.

#	**Nanoparticle Type**	**Code**
1	PHBV Nanoparticles	PHBV NP
2	PHBV NP conjugated with NLS	PHBV-NLS
3	PHBV NP loaded with DOX	PHBV-DOX
4	PHBV NP loaded with DOX and conjugated with NLS	PHBV-DOX-NLS

2.2.3.4. Cell Seeding and Uptake of Saos-2 Cells by Doxorubicin Loaded NLS Decorated Nanocapsules

Saos-2 cells were used in the *in vitro* studies to examine the uptake of Doxorubicin loaded NLS conjugated nanoparticles. The mechanism of EDC/ NHS crosslinking is explained in Appendix E. Before the cells were seeded, 200 μL nanosphere suspension (Doxorubicin loaded and NLS conjugated) (1 mg of NPs/ well) in PBS

(0.02 M, pH 7.4) was added onto sterile cover slips. Later, Saos-2 cells (20,000 cells/ well) were seeded onto the nanosphere suspension and placed in the wells of a 6-well plate (n=2) with their controls (no nanocapsules). Saos-2 cells were incubated in RPMI-1640 medium with 10% fetal bovine serum (FBS), 1% penicillin/streptomycin, 0.1% vancomycin and incubated at 37^{o}C in humidified CO_2 incubator (5% CO_2) for 24 h.

Cell cytoskeleton and nuclei were stained with FITC-Phalloidin (1:100 dilution in 0.1% PBS-BSA stock of 0.1 mg/ mL) (λ_{ex}: 532 nm, λ_{em}: 537-600 nm) or Alexa Fluor-Phalloidin (1:100 dilution in 0.1% PBS-BSA stock of 0.1 mg/mL) (λ_{ex}: 488 nm, λ_{em}: 525-600 nm) and Draq-5 (1:1000 dilution in PBS) (λ_{ex}: 647 nm, λ_{em}: 681-697 nm) or DAPI (λ_{ex}: 532 nm, λ_{em}: 605-635 nm) (1:100 dilution in 0.1% PBS-BSA solution), respectively. The dyes FITC-Phalloidin, Alexa Fluor-Phalloidin, DAPI and Draq-5 were used for the staining procedure.

After fixation with paraformaldehyde (1 mL, 4%, 15 min), cells were washed twice with 2 mL PBS and treated with Triton-X 100 in PBS (1 mL, 0.1%, v/v) at room temperature for 5 min. Afterwards, cells were washed twice with 2 mL PBS. BSA in PBS (1 mL, 1% w/v) was added onto the cells to reduce the non-specific binding of dyes and incubated for 30 min at 37^{o}C. After washing with 0.1% BSA solution twice, FITC-Phalloidin (1 mL) was added onto each cover slide and incubated at 37^{o}C for 1 h. After washing with PBS twice, Draq5 (1mL) was added onto each cover slide and incubated at room temperature for 30 min. Then, each well was washed with 1 mL PBS. Uptake of nanoparticles by Saos-2 cells was examined microscopically with Confocal Laser Scanning Microscopy (CLSM) (Leica DM2500, Germany).

2.2.3.5. Effect of Nile Red Loaded PHBV Nanoparticles on L929 Mouse Fibroblast Cells

L929 cells were used to determine the penetration and cytotoxic effect of PHBV nanoparticles on a healthy cell line. L929 cells (Passage no: 11) were cultured with DMEM high glucose medium that contained 10% fetal bovine serum (FBS) and 1% penicillin/streptomycin. They were incubated at 37^{o}C in humidified CO_2 incubator (5% CO_2) for 24 h until they reach confluency. Then, they were treated with trypsin-

EDTA solution (2 mL) for 5 min. The culture medium (4 mL) was added to the flask in order to inhibit the activity of trypsin. The cell suspension was centrifuged at 3000 rpm for 5 min in order to obtain the cell pellet. The cell pellet was resuspended in medium and counted by using a hemocytometer (Blau, Brand, Germany). 20,000 cells/ well were seeded onto 6 well plates. The staining procedure was carried out as in section 2.2.3.4.

CHAPTER 3

RESULTS AND DISCUSSION

3.1. Characterization of PHBV Nanocapsules

3.1.1. Morphology of PHBV Nanoparticles

Production of PHBV nanoparticles were carried out by using 10% (w/v) polymer solution in chloroform. The choice of this concentration was based on previous studies conducted with the same polymer (Yilgor et.al., 2009, Eke et.al., 2015). Scanning electron microscopy (SEM) images of PHBV nanocapsules are shown in Figure 24 and Figure 25. As expected, particles with nano size and smooth surfaces were formed. PHBV (HV content 11%) was used since it was available in our hand. The properties of the PHBV nanoparticles do not change by using a polymer with lower or higher valerate content, so PHBV with 11% HV content was used since it was available in our hand.

The average diameter of PHBV nanoparticles was found to be 206 ± 14 nm, 266 ± 12 nm and 319 ± 17 for unloaded (Figure 24), Doxorubicin and Nile Red loaded PHBV nanoparticles (Figure 25), respectively, using the SEM micrographs and ImageJ (NIH, USA) software. The diameter of the nanoparticles was measured by the application of the size measurement analysis of ImageJ software on SEM images.

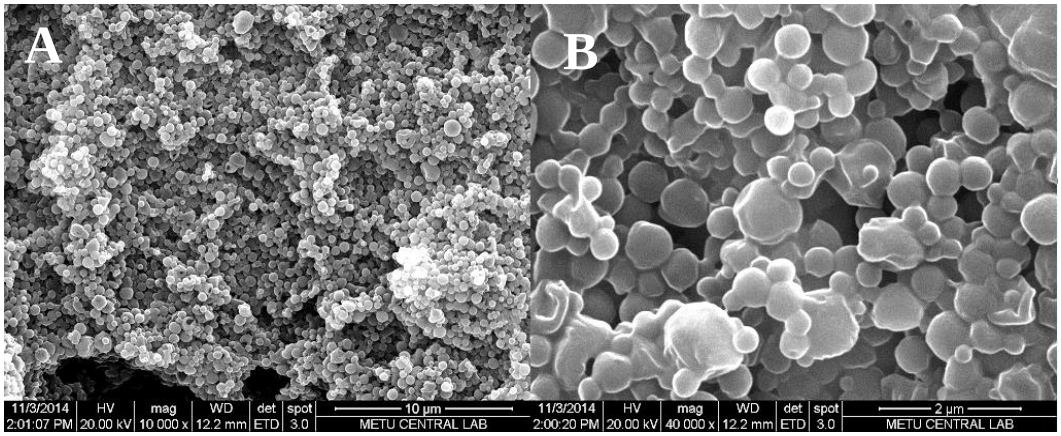

Figure 24: SEM images of unloaded PHBV nanoparticles. Magnification: a) x10,000, b) Same sample, higher magnification, x40,000.

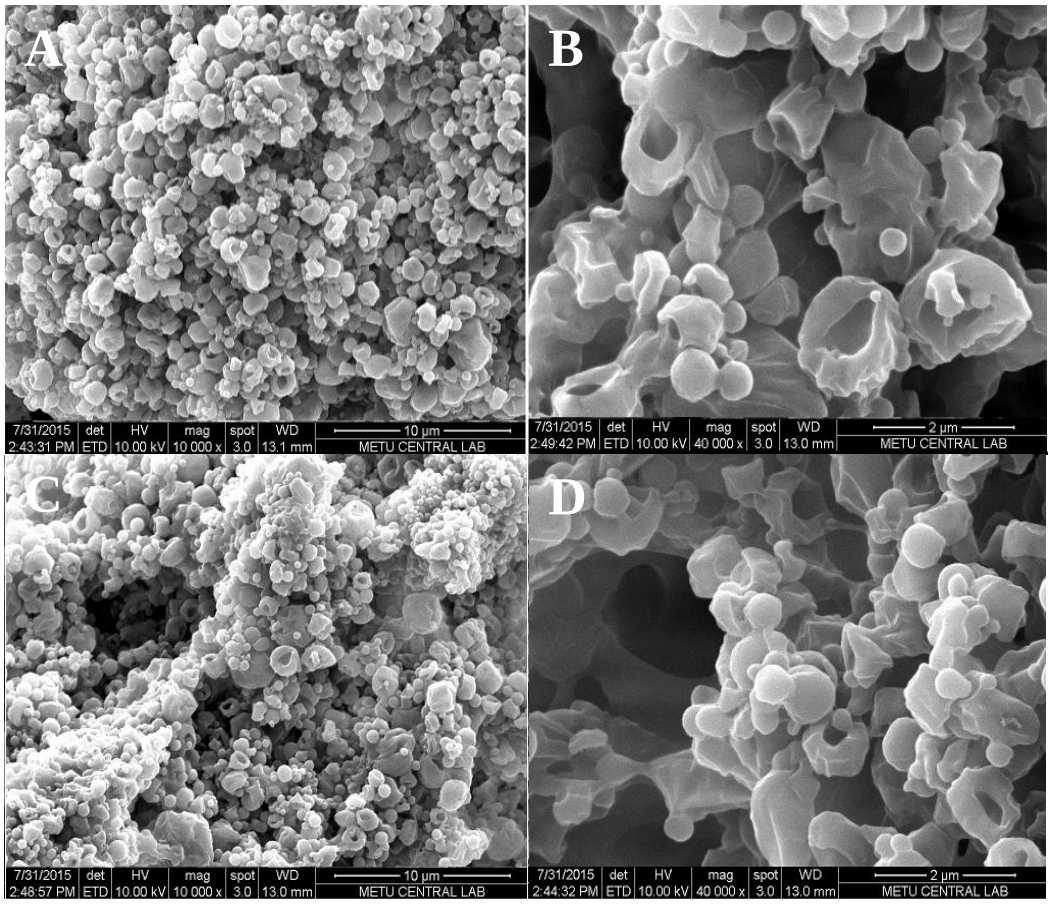

Figure 25: SEM images of PHBV nanoparticles. a) Nile Red loaded capsules (x10,000), b) Same sample, higher magnification (x40,000), c) Doxorubicin loaded capsules (x10,000), d) Same sample, higher magnification (x40,000).

3.1.2. Size Distribution of PHBV Nanocapsules

According to the data obtained with Malvern Zetasizer (Nano ZS90, UK), the average diameter of the unloaded PHBV nanocapsules were determined as 172 ± 2 nm whereas the average diameter of Doxorubicin and Nile Red loaded nanoparticles were 266 ± 5 nm and 302 ± 2 nm, respectively. The average diameter of NLS conjugated Doxorubicin loaded PHBV nanoparticles were 266 ± 5 nm showing that the nanoparticle size slightly increased due to the conjugation of NLS onto the surface. It can be observed that drug loading results in a slight increase in the dimension of PHBV nanoparticles. However, the difference in increase is not significant when it is compared between the particles that were loaded with Doxorubicin and Nile Red which were 266 ± 5 and 302 ± 2, respectively. According to Misra et.al., 2010, PLGA nanoparticles did not significantly increase in size after the conjugation of NLS onto the nanoparticle surface (226 nm vs 234 nm). The Doxorubicin loaded PHBV nanocapsules has an average diameter of 266 nm; however, since these nanoparticles are not monodisperse, there are also low dimensional ones up to 100 nm, so these smaller ones could be expected to be transferred into the nucleus.

3.1.3. Encapsulation Efficiency and Loading of Doxorubicin and Calcein

Encapsulation efficiency of active agents in PHBV nanocapsules were initially investigated by using Calcein as a molecular model molecule for Doxorubicin since its hydrophilicity and size (Mw: 622.53 g/mol) are similar to Doxorubicin (Mw: 579.98 g/mol). The encapsulation efficiencies of the particles for Calcein and Doxorubicin were quite similar (22.3±1.1 vs. 22.9±1.7) (Table 3). Thus, the use of Calcein as a substitute for Doxorubicin in the optimization steps appears to be very appropriate.

Table 3: Encapsulation efficiency and loading of Calcein and Doxorubicin in PHBV nanocapsules

Bioactive Agents	E. E. (%)	Loading (%)
Calcein	22.3±1.1	10.4±0.5
Doxorubicin	22.9±1.7	57.46±4.3

The loading of the drug, Doxorubicin, into the particles was achieved by water-in-oil-in-water emulsion technique where the drug was mostly encapsulated into the core of PHBV nanocapsules and some amount may be distributed through the polymeric membrane. The loading value for Doxorubicin was higher than Calcein (57.5 vs 10.4). Doxorubicin had a stock solution with a concentration of 1.7 mM whereas Calcein had 0.7 mM. Thus, although the encapsulation efficiency values were similar, since Doxorubicin had a higher concentration in stock solution meaning the amount of input was more, the amount of bioactive that was encapsulated in same amount of nanocapsules (20 mg) were expected to be more for Doxorubicin. In a recent study (Cui et.al., 2013), PLGA nanoparticles prepared by solvent evaporation and capsule loaded with Doxorubicin had an encapsulation efficiency of 22.0 ± 0.8% and loading of 31.0 ± 2.8% and these values are close to those obtained in this study. In solvent evaporation method, the solvent that was used to dissolve PLGA polymer was evaporated overnight, which is similar to the method in this study. In another recent study (Chittasupho et.al., 2014), Doxorubicin loaded PHBV nanoparticles were prepared by solvent displacement method and using sodium carboxymethyl cellulose as a surfactant and had an encapsulation efficiency of 74.0 ± 5.4% and loading of 7.9 ± 0.2%, however; the nanoparticles had a mean diameter of 396 ± 7 nm. This difference in encapsulation efficiencies can be due to the usage of a different method and presence of a surfactant in the preparation.

The percent of encapsulation values of the model molecule (Calcein) and the drug molecule (Doxorubicin) are in agreement with each other.

3.1.4. X-ray Photoelectron Spectroscopy (XPS) Analysis

PHBV nanocapsules with and without NLS were analyzed with XPS in order to determine the presence of NLS on nanoparticle surfaces. XPS analysis for NLS did not show the presence of N which would have come from NLS, a small oligopeptide composed of 20 amino acids (2361.9 g/mol) (Table 4). Thus, it was not possible to show the presence NLS on PHBV nanoparticles most probably due to the presence of very small quantity on the particles.

Table 4: Atomic percentage composition of nanoparticles.

Nanocapsule Type	**C**	**O**
Unconjugated	67.8	32.2
NLS conjugated	70.6	29.4

3.2. *In situ* Release of Doxorubicin from PHBV Nanocapsules

The release kinetics of Doxorubicin from PHBV nanocapsules was assessed by measuring the amount of Doxorubicin (λ_{ex}: 480 nm, λ_{em}: 590 nm) release into the medium by using spectrofluorometry. The data obtained was tested with the Higuchi as well as to the Zero and First Order Kinetics equations.

Zero order release model should yield a straight line when the amount of drug released versus time is plotted. It is calculated according to the following equation;

$M_t/M_\infty = k_0.t$……..….. (IV)

First order release model is represented by a straight line when $\ln M_t$ is plotted against time and rate constant calculated according to the following equation;

$M_t/M_\infty = e^{kt}$…….…… (V)

Higuchi release model is represented by the following equation;

$M_t/M_\infty = k_H.t^{1/2}$…….……... (VI)

In these equations; M_t is the amount of drug released at time t (h), M_∞ is the amount of drug released at time infinity (h), and k_0, k_1 and k_H are the rate constants for Zero order, First order and Higuchi models, respectively.

The *in situ* release behavior of Doxorubicin loaded PHBV nanocapsules is presented in the cumulative release (%) vs time plot (Figure 26). It is observed that the nanocapsules show a burst release of the encapsulated drug with a high release up to 20% in about 1 day. This burst release is possible due to the drug that is adsorbed or attached by other means on the surface of nanocapsules. The remaining drugs that were located inside the core of the nanocapsules were released later with Zero order at a constant rate (k= 0.167) (Table 5). In a previous study (Tewes et al., 2007), it was reported that Doxorubicin loaded PLGA nanoparticles that were prepared by single emulsion method released 63% of Doxorubicin in 60 days in a sustained release manner. In another study (Cui et al., 2013), magnetic silica nanoparticles carrying Doxorubicin and coated with PLGA showed a sustained release profile releasing 60% of its content in 5 days, probably fitting Higuchi equation. The data obtained in this study provided a more controlled release of DOX after a large burst.

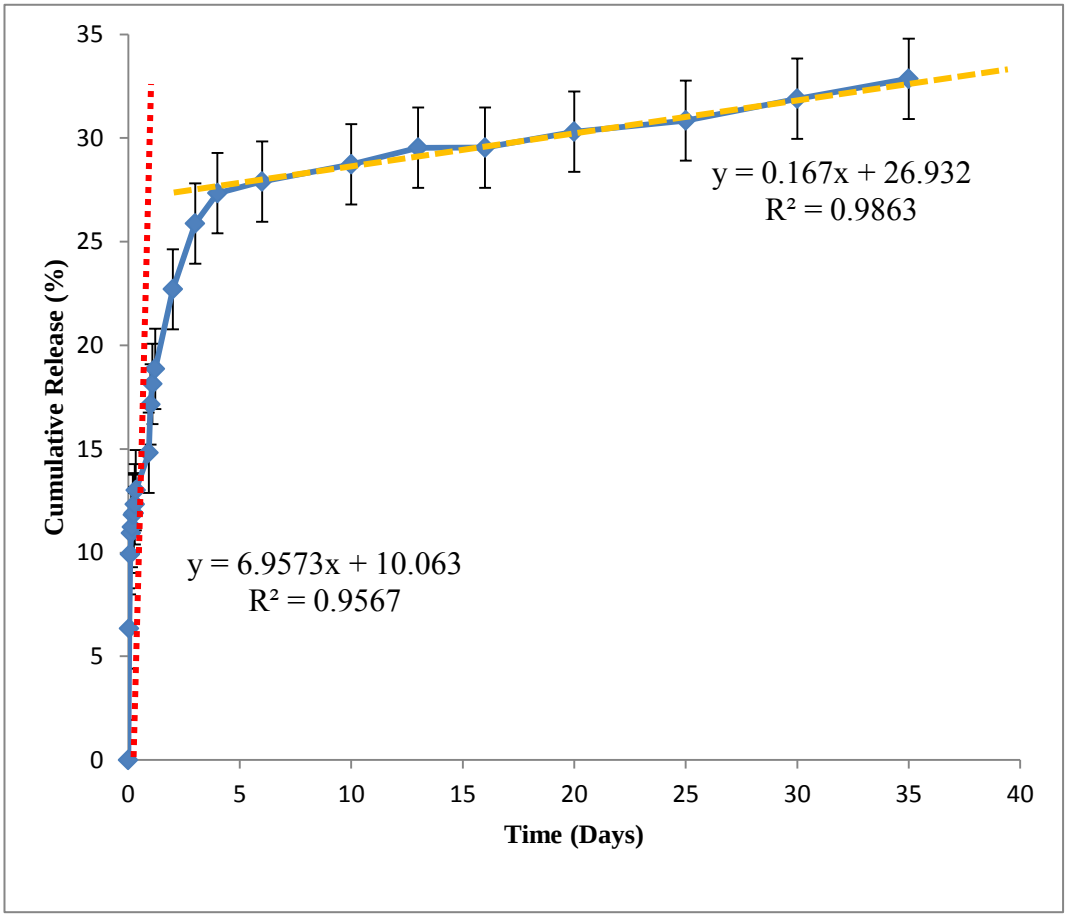

Figure 26: *In situ* release of Doxorubicin from PHBV nanoparticles into ultrapure water (n=3).

According to Figure 27, the release profile of Doxorubicin loaded PHBV nanocapsules do not fit the Higuchi model since the data does not yield a straight line. The data shows that the nanocapsules have a biphasic release profile or as Figure 26 shows a Burst followed by a Zero Order release.

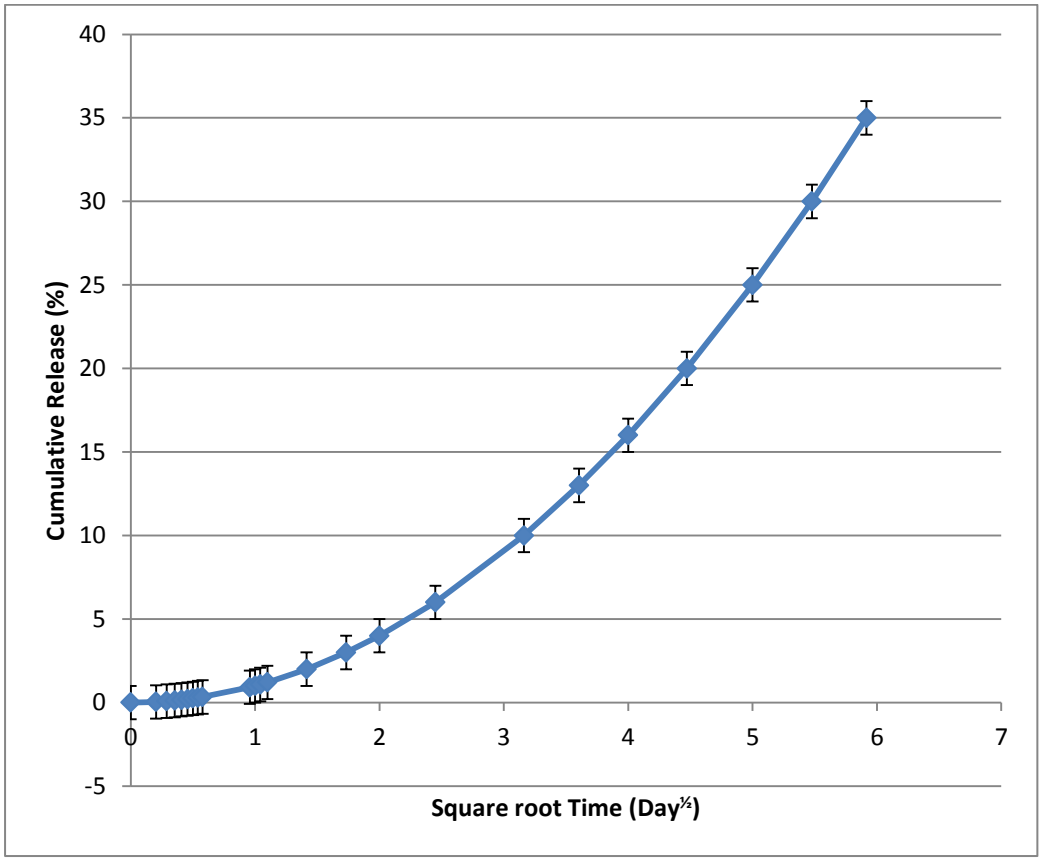

Figure 27: The Doxorubicin release profile according to Higuchi model.

Table 5: Kinetic analysis of Doxorubicin release from PHBV nanocapsules

Samples	Release Kinetics Model, Rate Constant (k) and r^2 values					
	Zero Order		First Order		Higuchi	
	k	r^2	k	r^2	k	r^2
Doxorubicin	0.167	0.98	6.21	0.70	1.19	0.83

3.3. *In vitro* Studies

3.3.1. Effect of Free Doxorubicin on Saos-2 Cell Proliferation

The effect of free Doxorubicin on Saos-2 cells were determined by preparing the final concentration in the range 0.01-100.0 µg/mL in the cell culture medium and the cell numbers were determined with Alamar Blue Cell Proliferation Assay on Day 4 (Figure 28).

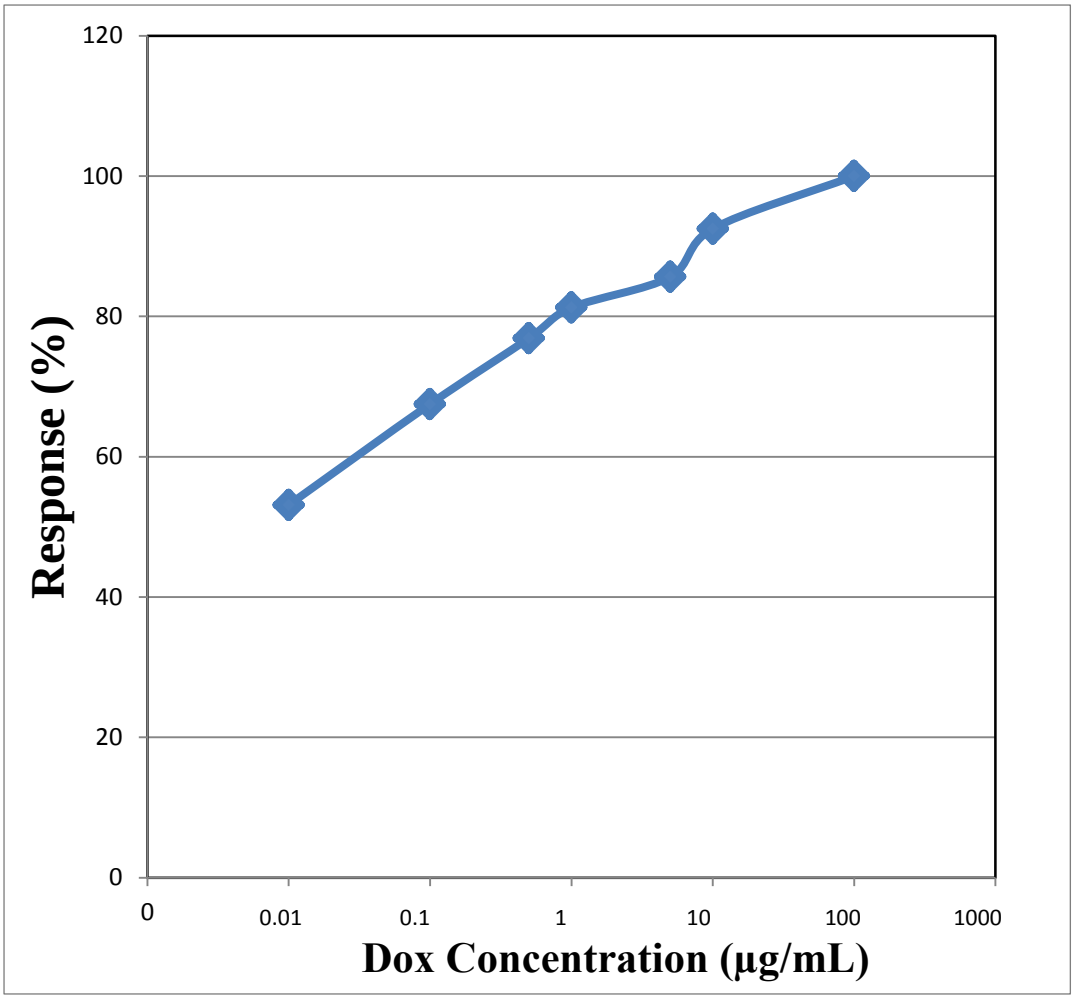

Figure 28: Effect of free Doxorubicin on Saos-2 cell proliferation measured using Alamar Blue test on Day 4 of exposure to the drug.

The results in Figure 28 show that doxorubicin has a significant antiproliferative effect on Saos-2 cells in a concentration dependent manner where the number of cells

decreases as the concentration of Doxorubicin increases from 0.01 to 100 μg/ mL. The cell seeding density was 20,000/ well and they were able to grow very slowly in the presence of the Doxorubicin doses of 0.01 to 10 μg/mL which correspond to 350 $\mu g/m^2$ – 350 mg/m^2 for human applications. Typical human dose is in this range. As reported by Mita et al., (2015), at 100 μg/mL dose (3.5 g/ m^2), Doxorubicin was extremely effective clinically.

3.3.2. Effect of Doxorubicin Carrying PHBV Nanocapsules on Saos-2 Cell Viability

The effect of nanoparticles on Saos-2 cell proliferation were determined using 4 groups of nanoparticles (NPs) (PHBV nanoparticles, PHBV nanoparticles conjugated with NLS, PHBV nanoparticles loaded with Doxorubicin, PHBV nanoparticles loaded with Doxorubicin and conjugated with NLS) and free Doxorubicin at a concentration of 0.6 μg/mL suspended in the cell culture medium. The cell numbers were determined with Alamar Blue Cell Proliferation Assay on Day 4 of exposure to Doxorubicin (Table 6 and Figure 29).

Table 6: Effect of PHBV nanoparticles carrying NLS and Doxorubicin on Saos-2 Cell Proliferation using Alamar Blue test on Day 4 of exposure to the drug.

Nanoparticle Concentration (4 mg/mL)	**Cell Number/Well ($x10^3$)***
Control (Only Cells) (no DOX)	199±2.4
PHBV NP (no DOX)	145±2.6
PHBV NP conjugated with NLS (no DOX)	152±0.8
PHBV NP loaded with DOX (0.58 μg)	63±1.5
PHBV NP loaded with DOX and conjugated with NLS (< 0.58 μg)	35±0.7
Free Doxorubicin (0.60 μg)	41±0.4

*Cell seeding density: 25,000 cells/well

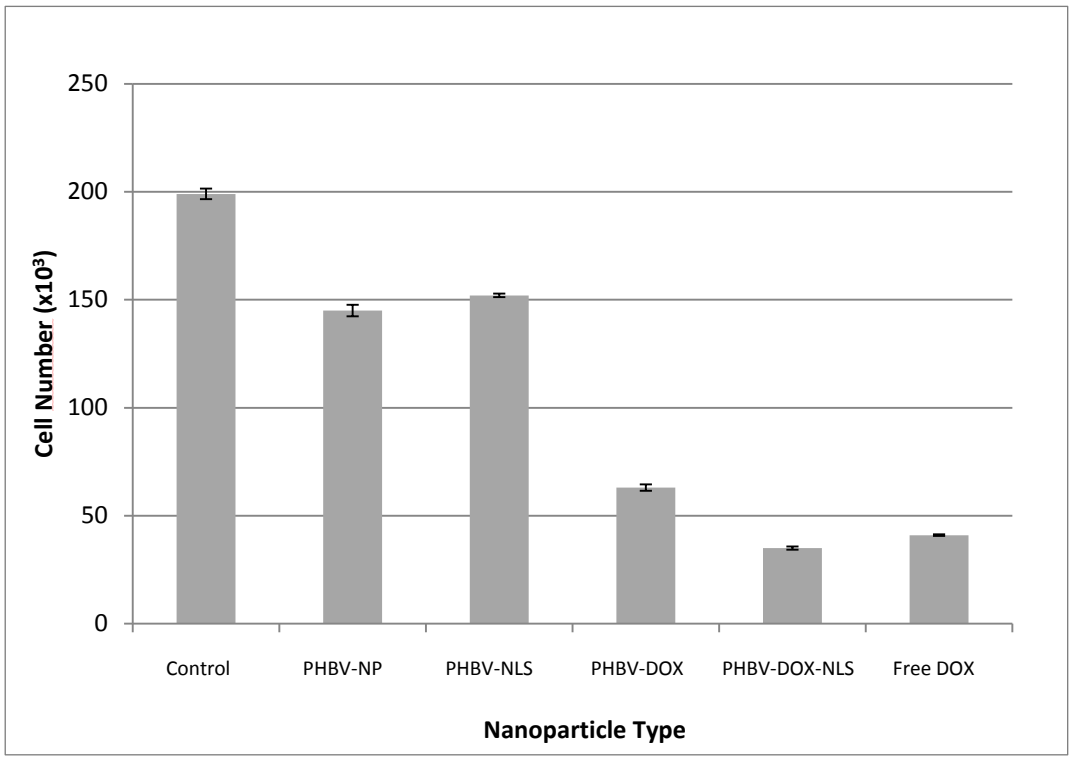

Figure 29: Effect of PHBV nanoparticles on Saos-2 proliferation (n=3). Results of Alamar Blue assay (Day 4).

In a previous *in vitro* study (Graat et al., 2006), it was found that IC_{50} for Doxorubicin on Saos-2 cell line was 37±16 nM, and this corresponded to 0.58 µg Doxorubicin. Based on this Reference, the Doxorubicin effectiveness tests were carried out where each sample carried 0.58 µg Doxorubicin per well of 25,000 cells. In our case, it was calculated that 4 mg/ mL PHBV nanoparticles contained 0.58 µg Doxorubicin. It can be deduced from the release data in section 3.2 that about 28% of Doxorubicin is released at the end of Day 4. Thus, it was decided to subject the Saos-2 cells to the nanoparticles with a dose of 4 mg nanocapsules/ mL for each group so that the nanoparticles would theoretically be able to release 0.58 µg by the end of day 4. It can be seen from Table 6 that control (no nanoparticle and no drug) group reached 199,000 cells on Day 4 starting with 25,000 cells seeded. PHBV nanoparticles and PHBV nanoparticles conjugated with NLS (PHBV-NLS) had 145,000 and 152,000 cells, respectively. Since the values are close to each other, it

can be concluded that PHBV nanoparticles cause a certain degree of decrease in cell growth but NLS conjugation did not have a significant additional effect on the cell numbers. PHBV nanoparticles that were loaded with Doxorubicin had 63,000 cells whereas PHBV nanoparticles that were loaded with Doxorubicin and conjugated with NLS had almost half, 35,000, cells. It can be deduced from these that conjugation with NLS has a significant impact on the delivery of Doxorubicin into nucleus which is the site where the drug shows its effect on the DNA. Free Doxorubicin with a concentration of 0.6 µg/ mL led to a cell number of 41,000 showing that free Doxorubicin has a high impact on the decrease in cell numbers. This value is more effective than Doxorubicin loaded nanoparticles and this can be because the nanoparticles did not release all their content in the Day 4 incubation so that the decrease in the cell number was less. When the cell numbers for Doxorubicin loaded, NLS conjugated PHBV nanocapsules and free Doxorubicin are compared (35,000 vs 41,000), it is observed that in the case where free Doxorubicin had applied a higher number of cells were obtained. Although the numbers are close, the difference can be because the delivery of the drug with NLS activated nanocapsules was more efficient compared to the transport of the free drug. Since the nanocapsules carry Doxorubicin inside the core, they prevent the drug molecules from the degradation or damaging by enzymes inside the lyso/endosomal vesicles or inside the cytoplasm. The drug molecules are also released in a sustained release mechanism from the nanocapsules. However, when the medium has free Doxorubicin, the drug molecules could be degraded by certain enzymes in the medium. The free Doxorubicin that was taken up by the Saos-2 cells may be directly thrown out from the cell membrane since they can be detected as cytotoxic from certain mechanisms inside the cell. They also could be degraded by the enzymes inside the cells. This explains the more efficient delivery of the drug by the PHBV nanocapsules when it is compared with the medium that contains free Doxorubicin molecules.

3.3.3. Influence of PHBV Nanocapsules on Adhesion and Proliferation of L929 Mouse Fibroblast Cells

L929 cells were seeded onto the slides that already contained a layer of PHBV nanocapsule suspension in order to study the effect of nanoparticles on the viability and spreading of the cells. Nile Red loaded PHBV nanocapsules were examined by fluorescence microscopy (Zeiss Axio Imager 2.0, Germany). Figure 30 A shows the differential interference contrast (DIC) image of L929 cells that were treated with Nile Red loaded PHBV nanocapsules where the nanoparticles can be observed. Figure 30 B and C shows the cell nuclei and the cytoplasm of L929 cells, respectively. Figure 30 D is an overlay of various images with different stains and shows that Nile Red loaded PHBV nanoparticles can be seen as blue specs indicating that they were able to cross the cell membrane successfully. The attachment of L929 cells onto the slide surface with their appendices and with no morphological change showed that the cells were alive. Thus, PHBV nanocapsules were not harmful to L929 cells (Figure 30).

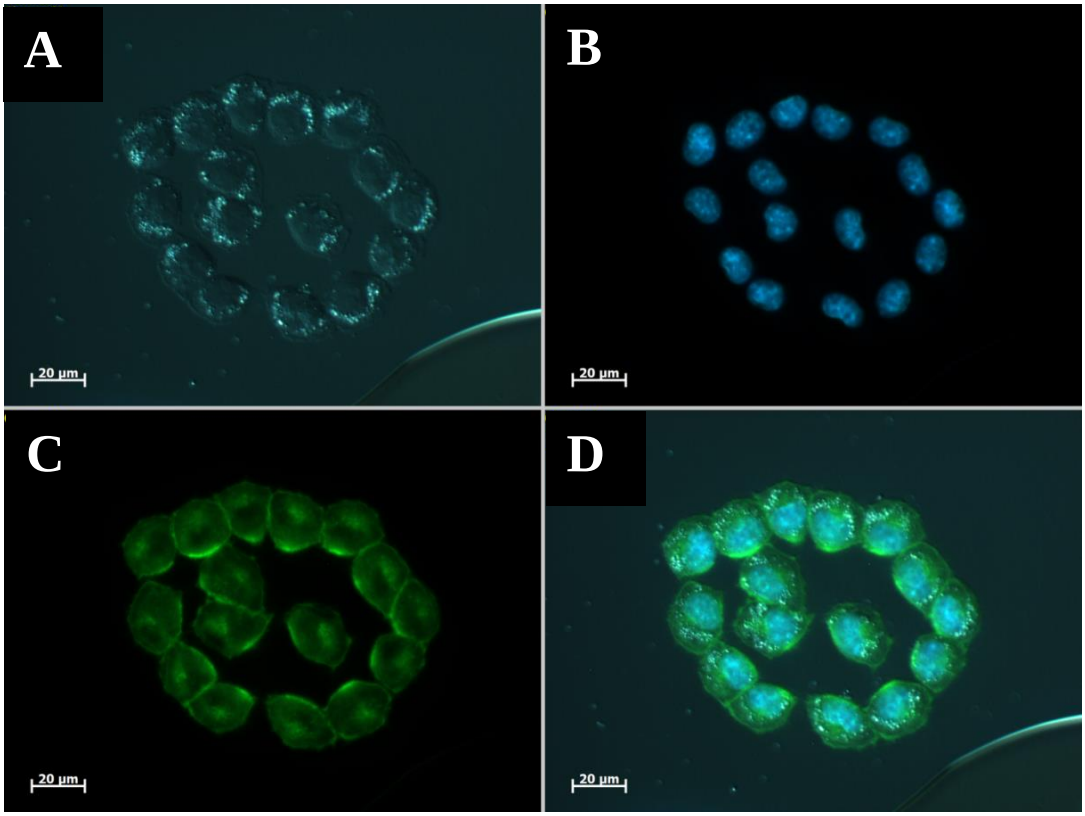

Figure 30: L929 human fibroblast cell attachment on the surface. L929 cells were seeded on PHBV nanospheres (2 mg/ mL) in a suspension. A) Differential interference contrast (DIC) image, B) Cell nuclei (stained with DAPI), C) Cell cytoskeleton (stained with FITC-Phalloidin), D) Overlay (composite) image showing all the components. The cells were incubated for 24 h.

3.3.4. Intracellular Localization of Nile Red Loaded PHBV Nanocapsules in Saos-2 Cells by Confocal Microscopy (CLSM)

PHBV nanocapsules were examined under the confocal laser scanning microscopy (CLSM) (Leica DM2500, Germany). All groups were incubated for 24 h. The control group of Saos-2 cells (Figure 31 A) was not treated with PHBV nanocapsules. The second group of Saos-2 cells (Figure 31 B) was treated with PHBV nanocapsules loaded with Nile Red to show the nanocapsules. The final group of Saos-2cells (Figure 31 C) was seeded with PHBV nanocapsules that were loaded with Nile Red

and conjugated with NLS. All groups were stained with FITC-Phalloidin and Draq5 to show the cytoskeleton and nucleus, respectively.

The control group (Figures 31 A, D and G) shows no nanoparticles or their stain Nile red since they were not treated with nanoparticle suspensions. The second group (Figures 31 B, E and H) shows that the nanocapsules were distributed throughout the cytoplasm without any particular localization in the absence of NLS signal and they were able to cross the cell membrane. According to Jans et. al. (2009), the transfer of nanoparticles across cell membranes depends on the particle size and hydrophobicity of the nanoparticle where mostly submicron sized nanoparticles with higher hydrophilicity are taken up. Sahoo et.al. (2010) stated that uptake by cells could be achieved by either phagocytosis or endocytosis where the nano-sized particles are transferred across the cell membrane by endocytosis. However, in the transfer to the nucleus, the nanoparticles must be targeted to the nuclear membrane of the nucleus by using a targeting agent, which was NLS in the present case. In the final group (Figure 31 C, F and I), it can be seen that Nile Red loaded and NLS conjugated PHBV nanocapsules were able to cross the cell membrane and surround the nucleus. This states that these nanocapsules are located around the nuclear membrane forming a ring and showing that NLS molecule was successful in targeting these nanocapsules too close to the nucleus. The nanoparticles, however, do not seem to have crossed the nuclear membrane which can be due to the relatively particle sizes (ca 302 nm) being relatively larger than the recommended values (ca. 50 nm). When Figure 31 E and F are compared, it can be clearly seen that in the absence of NLS, nanoparticles are distributed throughout the cytoplasm whereas in the presence of NLS, they were located close to the nucleus, localizing around the nuclear membrane in a targeted fashion.

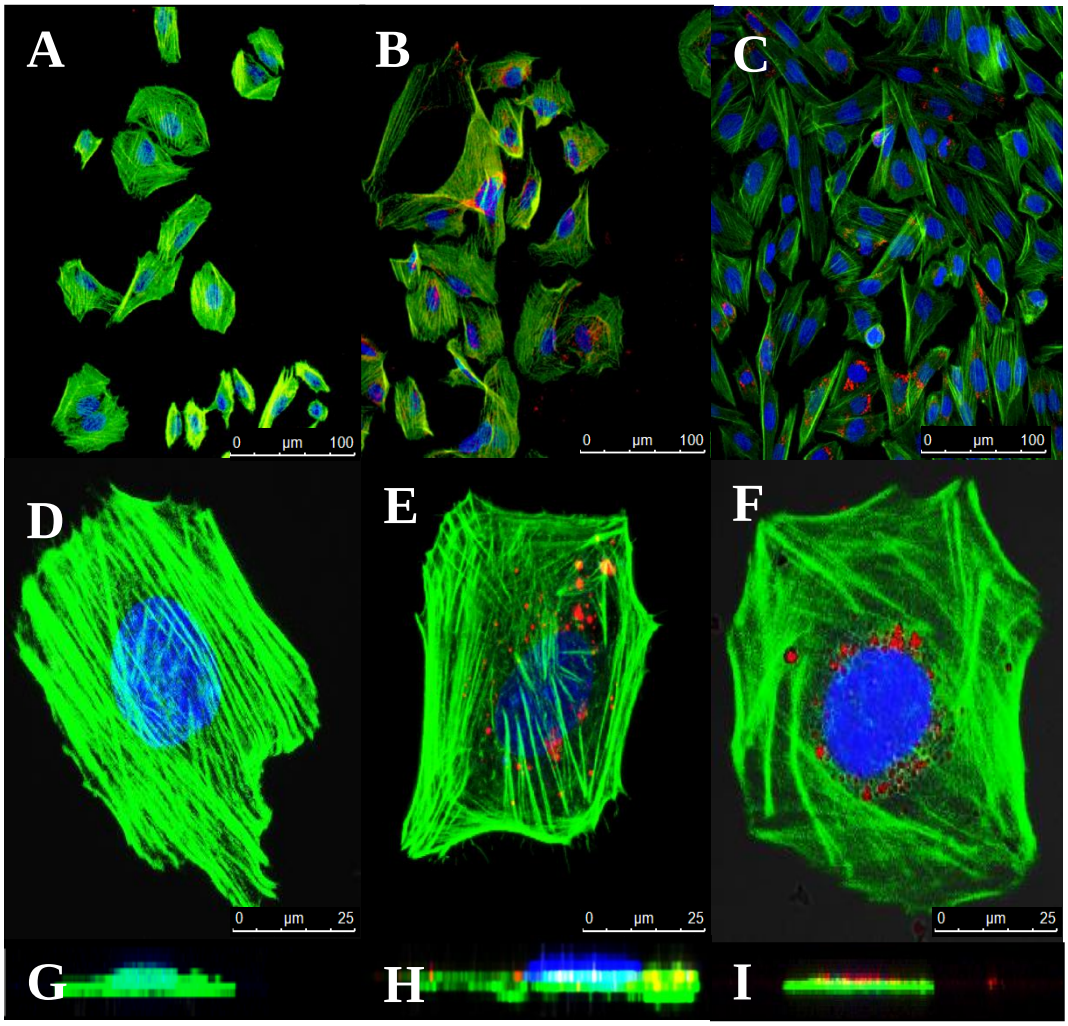

Figure 31: Confocal microscopy of the interaction of Nile Red loaded PHBV nanocapsules and Saos-2 Cells. A) Control (untreated) cells (x20), B) Cells treated with Nile Red loaded in PHBV nanocapsules (x20), C) Cells treated with Nile Red loaded and NLS conjugated PHBV nanocapsules. D, E and F are higher magnifications (x60) of A, B and C, respectively. G, H and I are z-stack images of D, E and F, respectively. The cells were stained with FITC-Phalloidin for the cytoskeleton and Draq5 for the nucleus and they were incubated for 24 h.

3.3.5. Intracellular Localization of Doxorubicin Loaded PHBV Nanocapsules in Saos-2 Cells by Confocal Microscopy (CLSM)

PHBV nanocapsules were examined under confocal laser scanning microscope (CLSM) (Leica DM2500, Germany). Saos-2 cells were incubated for 24 h. All groups were stained with Alexa Fluor 488-Phalloidin and Draq5 to show the cytoskeleton and nucleus, respectively. In section 3.3.6. confocal images of Nile Red loaded PHBV nanoparticles were shown. Nile Red stains the polymeric shell of PHBV nanoparticles because they are both hydrophobic. Thus, it was used as a fluorescent dye (λ_{ex}: 485 nm, λ_{em}: 525 nm) in order to locate the nanoparticles in the cell. It was seen that the nanocapsules were successful in crossing the cell membrane. Doxorubicin is a water soluble, anticancer drug which accumulates inside the nanocapsules (Figure 32). It shows that the drug was transferred through the cell membrane when encapsulated by the nanocapsule.

Confocal microscopy of Saos-2 cells treated with Doxorubicin loaded and NLS conjugated PHBV nanoparticles shows that nanoparticles successfully cross the cell membrane and accumulate around the nucleus (Figure 32). Clear distinction between cytoplasm, Doxorubicin loaded nanoparticles and the nucleus due to the stains, Alexa Fluor 488-Phalloidin, Doxorubicin autofluorescence and Draq 5, used enables us to see that nanoparticles accumulated around the membrane of the nucleus. This targeting of nanoparticles to the nuclear membrane is expected to result in a greater concentration of Doxorubicin around and in the nucleus. According to Tkachenko et al. (2004), NLS conjugated gold nanoparticles with a diameter of 20 nm were able to cross the nuclear membrane of HeLa cells with the help of their small size. In that study, nanoparticles were injected directly into the cytoplasm bypassing the cell membrane entry step. In another study (Cheng et. al., 2008), quantum dot carrying PLGA nanoparticles conjugated with NLS and with a diameter of 72 nm were taken up by HeLa cells and delivered into the nucleus. Lee et. al. (2005) demonstrated that PLGA coated iron oxide nanoparticles with a diameter of 115 nm were able to pass through the human mesenchymal stem cell membrane and delivered into the nucleus. However, in our study, Doxorubicin loaded and NLS conjugated PHBV

nanocapsules had a relatively larger size than recommended (ca 266 nm) a prevented them from passing through the nuclear membrane.

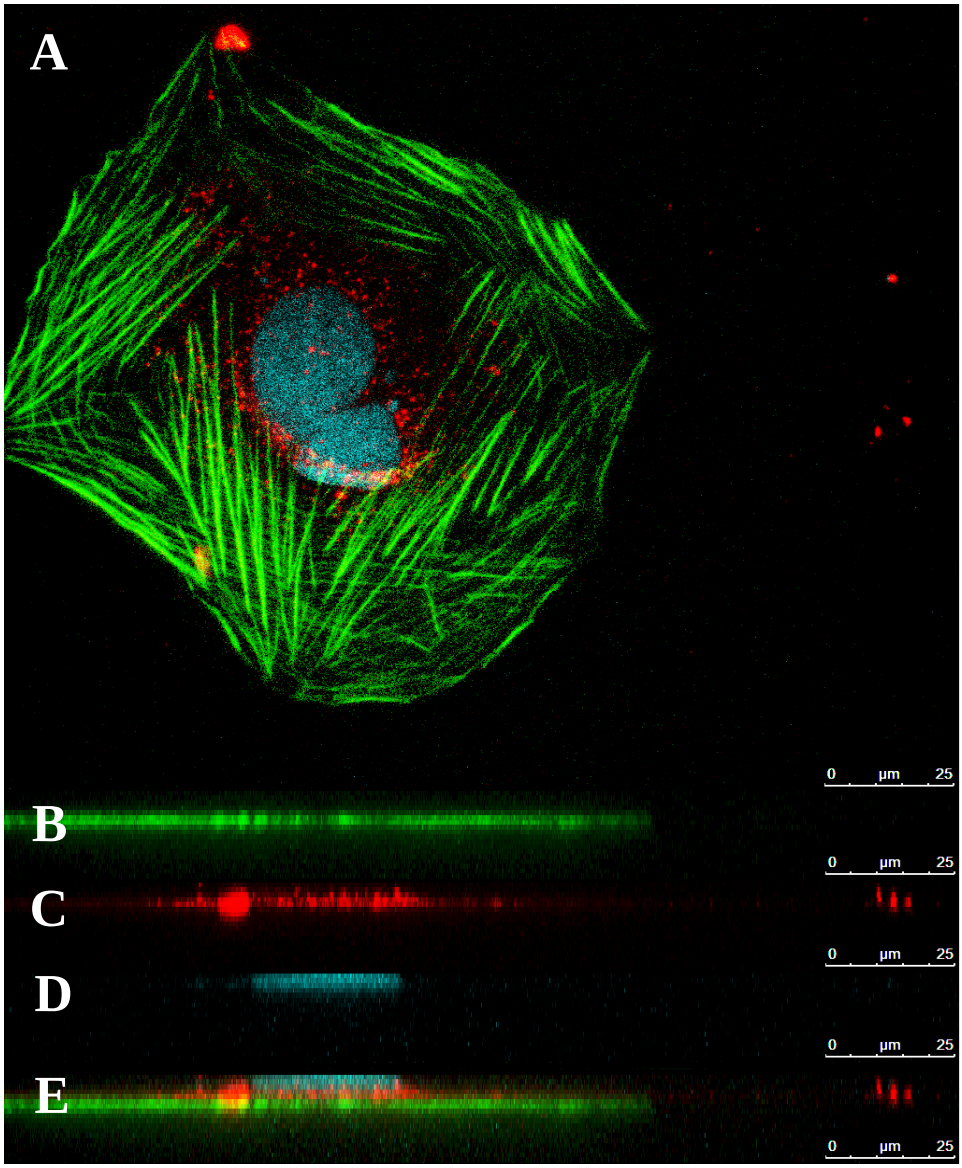

Figure 32: Confocal Microscopy images of Doxorubicin loaded PHBV nanoparticles (4 mg/ mL) in Saos-2 Cells. A) The overlay (composite) micrograph (x60). B) Z-stack of Cytoplasm, C) Z-stack of Doxorubicin loaded in PHBV nanoparticles, D) Z-stack of Nucleus, E) Z-stack of Overlay. The cells were stained with Alexa-Phalloidin for the cytoskeleton and Draq5 for the nucleus and they were incubated for 24 h.

3.3.6. The Effect of Doxorubicin Loaded NLS Conjugated PHBV Nanoparticles on Saos-2 Cells

Saos-2 cells were examined under the confocal laser scanning microscope (CLSM) (Leica DM2500, Germany). In section 3.3.2, it was observed that the cell numbers were similar for cells treated with free Doxorubicin and with Doxorubicin loaded and NLS conjugated PHBV nanoparticles (41,000 vs 35,000); this was less than cells treated with Doxorubicin loaded PHBV nanoparticles (63,000) showing the increased effectiveness of the nanocapsules due to targeting with NLS. In this section, the area of Saos-2 cells and the area of their nuclei of these 3 groups were compared by using Image J (NIH, USA) software on the confocal microscopy images (Table 7, Figure 33 and Figure 34).

Table 7: The areas of Saos-2 cells and their nuclei.

Sample Type	Area of Cell (μm^2)	Area of Cell Nuclei (μm^2)
Control (Only Cells)	1121	506
Free Doxorubicin	377	233
PHBV NP loaded with DOX	505	323
PHBV NP loaded with DOX and conjugated with NLS	358	126

The areas of the cells and the nuclei for Saos-2 cells that were not treated with PHBV nanoparticles (Figure 33 A) were 1121 and 506 μm^2, respectively. Upon treatment with free Doxorubicin, the values for the cells shown in Figure 33 B decreased to 377 and 233 μm^2, respectively. When Doxorubicin was loaded in PHBV nanocapsules (Figure 34 A), the effect was still strong (505 and 323 μm^2) and when Doxorubicin loaded NLS conjugated PHBV nanoparticles (Figure 34 B) were used, the highest effectiveness was observed (358 and 126 μm^2). This shows that the areas of Saos-2 cells were decreased significantly for the three groups carrying Doxorubicin and the Doxorubicin carrying NLS conjugated PHBV nanoparticles led to the lowest values. The area of cells as well as nuclei was the lowest for this group. This means that the targeting increased the effectiveness of the delivery of Doxorubicin and its toxic effect on Saos-2 cells.

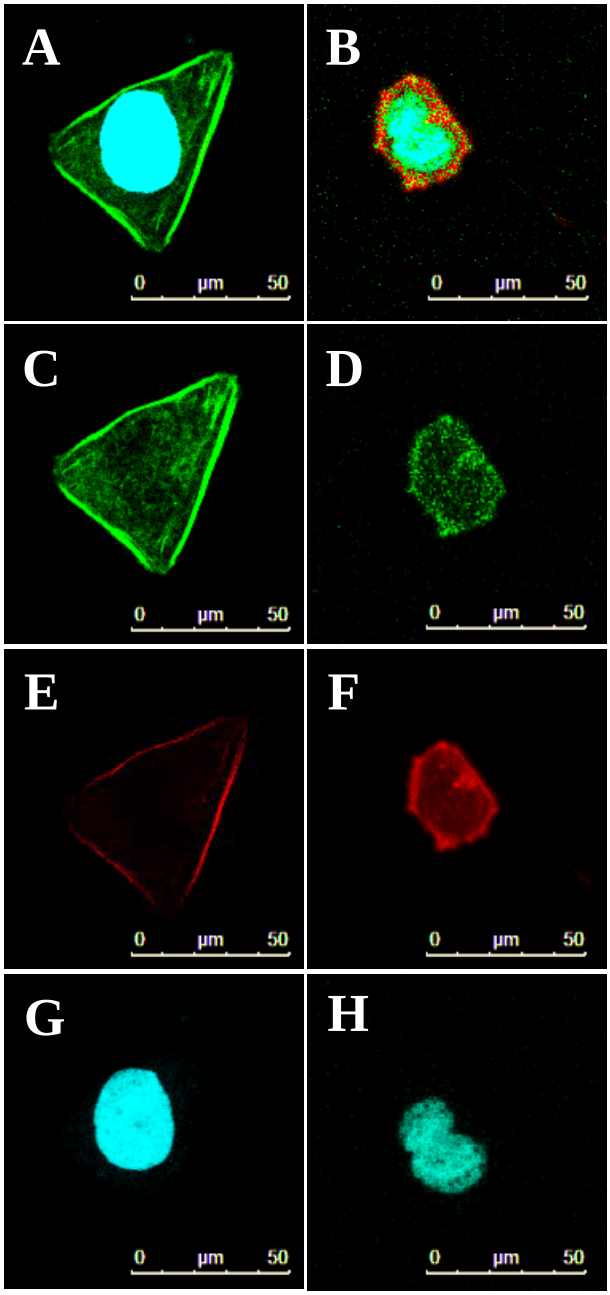

Figure 33: Confocal microscopy images of Doxorubicin carrying nanocapsules (4 mg/ mL) and Saos-2 cells. A) Control (untreated), B) Treated with free Doxorubicin. C and D are cytoplasm, E and F are Doxorubicin, G and H are nuclei of A and B, respectively (Magnification: 50x). The cells were stained with Alexa-Phalloidin and Draq5 to show the cytoskeleton and nucleus, respectively and they were incubated for 24 h.

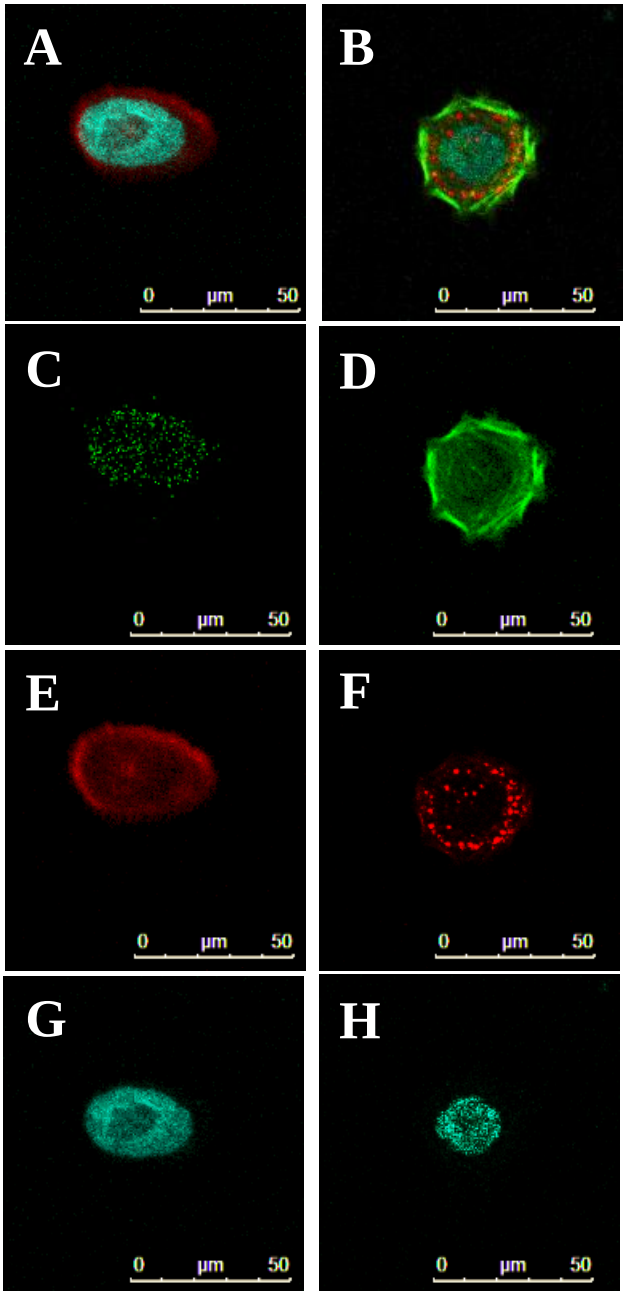

Figure 34: Confocal microscopy images of Doxorubicin carrying nanocapsules (4 mg/ mL) and Saos-2 cells. A cell treated with: A) Doxorubicin loaded PHBV nanocapsules, and B) Doxorubicin loaded and NLS conjugated PHBV nanocapsules. C and D show the cytoplasm, E and F show Doxorubicin, G and H show nuclei of A and B, respectively (Magnification: x50). The cells were stained with Alexa-Phalloidin and Draq5 to show the cytoskeleton and nucleus, respectively and incubated for 24 h.

In Figure 35, it is observed that the cell membrane of Saos-2 cells have gaps in them (indicated with red arrow). This probably indicates that Doxorubicin was effectively delivered into the nucleus by NLS conjugated PHBV nanocapsules in 24 h. The main action of Doxorubicin on cancer cells is based on Topoisomerase II inhibition which causes the generation of free radicals. These free radicals damage proteins, DNA and the cell membrane inducing an apoptosis through DNA cleavage and hydrogen peroxide formation (Wang et al., 2004, Mizutani et.al., 2005). According to the literature, since the cells cannot go through cell replication due to the intercalation of DNA by Doxorubicin, they may have gone through necrosis or apoptosis, since the cell membrane was disrupted as shown in Figure 35. The actual process can be further analyzed by using an apoptosis assay. However, from these results which shows a significant decrease in their number and deformation in cell shape, it can be stated that Doxorubicin was cytotoxic to the cells.

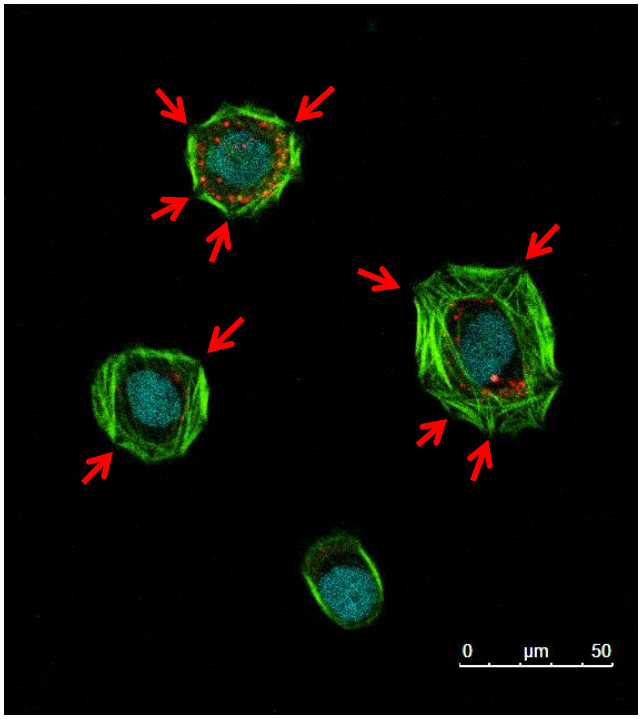

Figure 35: Confocal micrographs of Doxorubicin carrying and NLS conjugated PHBV nanocapsules (4 mg/ mL) and Saos-2 cells after 24 h incubation. The cells were stained with Alexa Fluor 488-Phalloidin and Draq5 to show the cytoskeleton and nucleus, respectively (Magnification: x50).

CHAPTER 4

CONCLUSION

In this study, PHBV nanocapsules were loaded with Doxorubicin and conjugated with NLS in order to target the nanoparticles carrying Doxorubicin to the nuclear membrane.
The drug release study indicated that the nanocapsules showed a burst release followed by a zero order release as expected from their being in capsule form.

The effect of Doxorubicin on Saos-2 cells was studied by Alamar Blue cell proliferation Assay and the results indicated that the antiproliferative effect of Doxorubicin increased with an increase in Doxorubicin concentration.

Confocal microscopy results showed that both Nile Red loaded NLS conjugated PHBV nanocapsules with and without Doxorubicin were able to cross the cell membrane and locate around the cell nucleus. This showed that the NLS molecule was successful in targeting the nanoparticles to the nuclear membrane increasing the efficiency of delivering Doxorubicin to the nucleus. The nanoparticles did not seem to cross this membrane, which is most probably due to the relatively large particle size (ca 265 nm) for penetration using the nuclear pores. The next step can be carrying the similar experiments by using smaller (~ 100 nm) particles and observe if these particles can achieve higher efficiency in the delivery of Doxorubicin.

REFERENCES

Akbarzadeh, A., Rezaei-Sadabady, R., Davaran, S., Joo, S. W., Zarghami, N., Hanifehpour, Y., Nejati-Koshki, K. (2013). Liposome: classification, preparation, and applications. Nanoscale Research Letters, 8(1), 102. doi:10.1186/1556-276X-8-102

Aulton, M. E., & Taylor, K. (2013). Aulton's Pharmaceutics: The Design and Manufacture of Medicines. Churchill Livingstone/Elsevier. Retrieved from https://books.google.com.tr/books?id=rrtGKQxcoWIC

Bahcecioglu, G., Buyuksungur, Kiziltay, Hasirci, N., & Hasirci, V. (2014). Construction and *in vitro* testing of a multilayered, tissue-engineered meniscus. Journal of Bioactive and Compatible Polymers, 29(3), 235–253. doi:10.1177/0883911514529688

Bangham, A. D., Standish, M. M., Watkins, J. C., & Weissmann, G. (1967). The diffusion of ions from a phospholipid model membrane system. Protoplasma, 63(1-3), 183–187. doi:10.1007/BF01248030

Belting, M., Sandgren, S., & Wittrup, A. (2005). Nuclear delivery of macromolecules: barriers and carriers. Advanced Drug Delivery Reviews, 57(4), 505–27. doi:10.1016/j.addr.2004.10.004

Bertrand, N., Wu, J., Xu, X., Kamaly, N., & Farokhzad, O. C. (2014). Cancer nanotechnology: The impact of passive and active targeting in the era of modern cancer biology. Advanced Drug Delivery Reviews, 66, 2–25. doi:10.1016/j.addr.2013.11.009

Biju, V., Mundayoor, S., Omkumar, R. V., Anas, A., & Ishikawa, M. (2010). Bioconjugated quantum dots for cancer research: Present status, prospects and remaining issues. Biotechnology Advances, 28(2), 199–213. doi:10.1016/j.biotechadv.2009.11.007

Biswas, S., & Torchilin, V. P. (2013). Nanopreparations for organelle-specific delivery in cancer. doi:10.1016/j.addr.2013.11.004

Biswas, S., & Torchilin, V. P. (2013). Nanopreparations for organelle-specific delivery in cancer. Advanced Drug Delivery Reviews. doi:10.1016/j.addr.2013.11.004

Bitounis, D., Fanciullino, R., Iliadis, A., & Ciccolini, J. (2012). Optimizing Druggability through Liposomal Formulations: New Approaches to an Old Concept. ISRN Pharmaceutics, 2012, 1–11. doi:10.5402/2012/738432

Bomsel, M., Tudor, D., Drillet, A. S., Alfsen, A., Ganor, Y., Roger, M. G., Fleury, S. (2011). Immunization with HIV-1 gp41 Subunit Virosomes Induces Mucosal Antibodies Protecting Nonhuman Primates against Vaginal SHIV Challenges. Immunity, 34(2), 269–280. doi:10.1016/j.immuni.2011.01.015

Cech, P. G., Aebi, T., Abdallah, M. S., Mpina, M., Machunda, E. B., Westerfeld, N., Abdulla, S. (2011). Virosome-formulated plasmodium falciparum AMA-1 & CSP derived peptides as malaria vaccine: Randomized phase 1b trial in semi-immune adults & children. PLoS ONE, 6(7). doi:10.1371/journal.pone.0022273

Chen, G. Q., & Wu, Q. (2005). The application of polyhydroxyalkanoates as tissue engineering materials. Biomaterials, 26(33), 6565–6578. doi:10.1016/j.biomaterials.2005.04.036

Chen, Y. J., Huang, Y. C., & Lee, C. Y. (2014). Production and characterization of medium-chain-length polyhydroxyalkanoates by Pseudomonas mosselii TO7.

Journal of Bioscience and Bioengineering, 118(2), 145–152. doi:10.1016/j.jbiosc.2014.01.012

Cheng, F. Y., Wang, S. P. H., Su, C. H., Tsai, T. L., Wu, P. C., Shieh, D. Bin, Yeh, C. S. (2008). Stabilizer-free poly(lactide-co-glycolide) nanoparticles for multimodal biomedical probes. Biomaterials, 29(13), 2104–2112. doi:10.1016/j.biomaterials.2008.01.010

Chittasupho, C., Lirdprapamongkol, K., Kewsuwan, P., & Sarisuta, N. (2014). Targeted delivery of doxorubicin to A549 lung cancer cells by CXCR4 antagonist conjugated PLGA nanoparticles. European Journal of Pharmaceutics and Biopharmaceutics : Official Journal of Arbeitsgemeinschaft Fur Pharmazeutische Verfahrenstechnik e.V, 88(2), 529–538. doi:10.1016/j.ejpb.2014.06.020

Choron, R. L., Chang, S., Khan, S., Villalobos, M., Zhang, P., Carpenter, J. P., Liu, Y. (2015). Paclitaxel impairs adipose stem cell proliferation and differentiation. Journal of Surgical Research, 196(2), 404–415. doi:10.1016/j.jss.2015.03.026

Choudhary, V., & Gupta, A. (2001). Polymer/Carbon Nanotube Nanocomposites, Carbon Nanotubes - Polymer Nanocomposites. Dr. Siva Yellampalli (Ed.), doi:10.5772/18423.

Ciesielski, S., Możejko, J., & Pisutpaisal, N. (2014). Plant oils as promising substrates for polyhydroxyalkanoates production. Journal of Cleaner Production, 106, 408–421. doi:10.1016/j.jclepro.2014.09.040

Crucho, C. I. C., & Barros, M. T. (2015). Formulation of Functionalized PLGA polymeric nanoparticles for targeted drug delivery. Polymer, 68, 41–46. doi:10.1016/j.polymer.2015.04.083

Cui, Y., Xu, Q., Chow, P. K. H., Wang, D., & Wang, C. H. (2013). Transferrin-conjugated magnetic silica PLGA nanoparticles loaded with doxorubicin and

paclitaxel for brain glioma treatment. Biomaterials, 34(33), 8511–8520. doi:10.1016/j.biomaterials.2013.07.075

Dasari, S., & Bernard Tchounwou, P. (2014). Cisplatin in Cancer therapy: Molecular mechanisms of action. European Journal of Pharmacology, 740, 364–378. doi:10.1016/j.ejphar.2014.07.025

De Villiers, M. M., Aramwit, P., & Kwon, G. S. (2009). Nanotechnology in drug delivery, 662. doi:10.1007/978-0-387-77667-5

Deng, C., Jiang, Y., Cheng, R., Meng, F., & Zhong, Z. (2012). Biodegradable polymeric micelles for targeted and controlled anticancer drug delivery: Promises, progress and prospects. Nano Today, 7(5), 467–480. doi:10.1016/j.nantod.2012.08.005

Düzgüneş, N., & Gregoriadis, G. (2005). Liposomes. Methods in Enzymology (Vol. 391). Elsevier. doi:10.1016/S0076-6879(05)91029-X

Eke, G., Goni-de-Cerio, F., Suarez-Merino, B., Hasirci, N., & Hasirci, V. (2015). Biocompatibility of Dead Sea Water and retinyl palmitate carrying poly(3-hydroxybutyrate-co-3-hydroxyvalerate) micro/nanoparticles designed for transdermal skin therapy. Journal of Bioactive and Compatible Polymers. doi:10.1177/0883911515585183

Elgadir, M. A., Uddin, M. S., Ferdosh, S., Adam, A., Chowdhury, A. J. K., & Sarker, M. Z. I. (2014). Impact of chitosan composites and chitosan nanoparticle composites on various drug delivery systems: A review. Journal of Food and Drug Analysis, 1–11. doi:10.1016/j.jfda.2014.10.008

Elzoghby, A. O. (2013). Gelatin-based nanoparticles as drug and gene delivery systems: Reviewing three decades of research. Journal of Controlled Release, 172(3), 1075–1091. doi:10.1016/j.jconrel.2013.09.019

Fanun, M. (2012). Microemulsions as delivery systems. Current Opinion in Colloid and Interface Science, 17(5), 306–313. doi:10.1016/j.cocis.2012.06.001

Florea, A.-M., & Büsselberg, D. (2011). Cisplatin as an Anti-Tumor Drug: Cellular Mechanisms of Activity, Drug Resistance and Induced Side Effects. Cancers, 3(1), 1351–1371. doi:10.3390/cancers3011351

Gasiorowski, J. Z., & Dean, D. a. (2003). Mechanisms of nuclear transport and interventions. Advanced Drug Delivery Reviews, 55(6), 703–16. Retrieved from http://www.ncbi.nlm.nih.gov/pubmed/12788535

Glück, U., Gebbers, J. O., & Glück, R. (1999). Phase 1 evaluation of intranasal virosomal influenza vaccine with and without Escherichia coli heat-labile toxin in adult volunteers. Journal of Virology, 73(9), 7780–7786.

Graat, H. C. a, Witlox, M. a, Schagen, F. H. E., Kaspers, G. J. L., Helder, M. N., Bras, J., … van Beusechem, V. W. (2006). Different susceptibility of osteosarcoma cell lines and primary cells to treatment with oncolytic adenovirus and doxorubicin or cisplatin. British Journal of Cancer, 94, 1837–1844. doi:10.1038/sj.bjc.6603189

Gregoriadis, G. (1973). Drug entrapment in liposomes. FEBS Letters, 36(3), 292–296. doi:10.1016/0014-5793(73)80394-1

Gregoriadis, G. (1976). The Carrier Potential of Liposomes in Biology and Medicine. New England Journal of Medicine, 295(14), 765–770. doi:10.1056/NEJM197609302951406

Gupta, R., Shea, J., Scafe, C., Shurlygina, A., & Rapoport, N. (2015). Polymeric micelles and nanoemulsions as drug carriers: Therapeutic efficacy, toxicity, and drug resistance. Journal of Controlled Release, 212, 70–77. doi:10.1016/j.jconrel.2015.06.019

Gürsel, I., & Hasirci, V. (1995). Properties and drug release behaviour of poly(3-hydroxybutyric acid) and various poly(3-hydroxybutyrate-hydroxyvalerate)

copolymer microcapsules. Journal of Microencapsulation, 12(2), 185–193. doi:10.3109/02652049509015289

Hasirci, N. (2007). Micro and Nano Systems in Biomedicine and Drug Delivery. Nanomaterials and Nanosystems for Biomedical Applications, 1–26. Retrieved from http://dx.doi.org/10.1007/978-1-4020-6289-6_1

Heath, J. R., Heath, J. R., Davis, M. E., & Davis, M. E. (2008). Nanotechnology and cancer. Annual Review of Medicine, 59, 251–65. doi:10.1146/annurev.med.59.061506.185523

Higuchi, T. (1961). Rate of release of medicaments from ointment bases containing drugs in suspension. Journal of Pharmaceutical Sciences, 50, 874–875. doi:10.1248/cpb.23.3288

Hillery, A. M., Lloyd, A. W., & Swarbrick, J. (2003). Drug Delivery and Targeting: For Pharmacists and Pharmaceutical Scientists. Taylor & Francis. Retrieved from https://books.google.com.tr/books?id=RCmK8BM2URUC

Hofmann, F. B., Board, E., Beavo, J. a, Busch, a, Ganten, D., Michel, M. C., Rosenthal, W. (2011). Handbook of Experimental Pharmacology: Methylxanthines (Vol. 197). doi:10.1007/978 3 642 13443 2

Kaminskas, L. M., McLeod, V. M., Kelly, B. D., Sberna, G., Boyd, B. J., Williamson, M., Porter, C. J. H. (2012). A comparison of changes to doxorubicin pharmacokinetics, antitumor activity, and toxicity mediated by PEGylated dendrimer and PEGylated liposome drug delivery systems. Nanomedicine: Nanotechnology, Biology, and Medicine, 8(1), 103–111. doi:10.1016/j.nano.2011.05.013

Kamphuis, T., Meijerhof, T., Stegmann, T., Lederhofer, J., Wilschut, J., & de Haan, A. (2012). Immunogenicity and protective capacity of a virosomal respiratory syncytial virus vaccine adjuvanted with monophosphoryl lipid a in mice. PLoS ONE, 7(5). doi:10.1371/journal.pone.0036812

Kim, K. Y. (2007). Nanotechnology platforms and physiological challenges for cancer therapeutics. Nanomedicine: Nanotechnology, Biology, and Medicine, 3(2), 103–110. doi:10.1016/j.nano.2006.12.002

Kompella, U. B., Amrite, A. C., Pacha Ravi, R., & Durazo, S. A. (2013). Nanomedicines for back of the eye drug delivery, gene delivery, and imaging. Progress in Retinal and Eye Research, 36, 172–198. doi:10.1016/j.preteyeres.2013.04.001

Krebs, A., Goldie, K. N., & Hoenger, A. (2005). Structural rearrangements in tubulin following microtubule formation. EMBO Reports, 6(3), 227–232. doi:10.1038/sj.embor.7400360

Lee, J. H., & Yeo, Y. (2015). Controlled drug release from pharmaceutical nanocarriers. Chemical Engineering Science, 125, 75–84. doi:10.1016/j.ces.2014.08.046

Lee, S. J., Jeong, J. R., Shin, S. C., Huh, Y. M., Song, H. T., Suh, J. S., Kim, J. D. (2005). Intracellular translocation of superparamagnetic iron oxide nanoparticles encapsulated with peptide-conjugated poly(D,L lactide-co-glycolide). Journal of Applied Physics, 97(10), 6–9. doi:10.1063/1.1853933

Leong, Y. K., Show, P. L., Ooi, C. W., Ling, T. C., & Lan, J. C. W. (2014). Current trends in polyhydroxyalkanoates (PHAs) biosynthesis: Insights from the recombinant Escherichia coli. Journal of Biotechnology, 180(2014), 52–65. doi:10.1016/j.jbiotec.2014.03.020

Li, Y., Wang, J., Wientjes, M. G., & Au, J. L.-S. (2012). Delivery of nanomedicines to extracellular and intracellular compartments of a solid tumor. Advanced Drug Delivery Reviews, 64(1), 29–39. doi:10.1016/j.addr.2011.04.006

Lu, Y., & Park, K. (2013). Polymeric micelles and alternative nanonized delivery vehicles for poorly soluble drugs. International Journal of Pharmaceutics, 453(1), 198–214. doi:10.1016/j.ijpharm.2012.08.04

Makadia, H. K., & Siegel, S. J. (2011). Poly Lactic-co-Glycolic Acid (PLGA) as biodegradable controlled drug delivery carrier. Polymers, 3(3), 1377–1397. doi:10.3390/polym3031377

Marchisio, P., Cavagna, R., Maspes, B., Gironi, S., Esposito, S., Lambertini, L., Principi, N. (2002). Efficacy of intranasal virosomal influenza vaccine in the prevention of recurrent acute otitis media in children. Clinical Infectious Diseases : An Official Publication of the Infectious Diseases Society of America, 35(2), 168–174. doi:10.1086/341028

Minko, T., Rodriguez-Rodriguez, L., & Pozharov, V. (2013). Nanotechnology approaches for personalized treatment of multidrug resistant cancers. Advanced Drug Delivery Reviews, 65(13-14), 1880–1895. doi:10.1016/j.addr.2013.09.017

Misra, R., & Sahoo, S. K. (2010). Intracellular trafficking of nuclear localization signal conjugated nanoparticles for cancer therapy. European Journal of Pharmaceutical Sciences, 39(1-3), 152–63. doi:10.1016/j.ejps.2009.11.010

Mita, M. M., Natale, R. B., Wolin, E. M., Laabs, B., Dinh, H., Wieland, S., Mita, A. C. (2015). Pharmacokinetic study of aldoxorubicin in patients with solid tumors. Investigational New Drugs, 33(2), 341–348. doi:10.1007/s10637-014-0183-5

Mizutani, H., Tada-Oikawa, S., Hiraku, Y., Kojima, M., & Kawanishi, S. (2005). Mechanism of apoptosis induced by doxorubicin through the generation of hydrogen peroxide. Life Sciences, 76(13), 1439–1453. doi:10.1016/j.lfs.2004.05.040

Mora-Huertas, C. E., Fessi, H., & Elaissari, A. (2010). Polymer-based nanocapsules for drug delivery. International Journal of Pharmaceutics, 385(1-2), 113–142. doi:10.1016/j.ijpharm.2009.10.018

Nie, S., Xing, Y., Kim, G. J., & Simons, J. W. (2007). Nanotechnology applications in cancer. Annual Review of Biomedical Engineering, 9, 257–288. doi:10.1146/annurev.bioeng.9.060906.152025

Okitsu, S. L., Silvie, O., Westerfeld, N., Curcic, M., Kammer, A. R., Mueller, M. S., Pluschke, G. (2007). A virosomal malaria Peptide vaccine elicits a longlasting sporozoite-inhibitory antibody response in a phase 1a clinical trail. PLoS ONE, 2(12). doi:10.1371/journal.pone.0001278

Orive, G., Gascón, A. R., Hernández, R. M., Domínguez-Gil, A., & Pedraz, J. L. (2004). Techniques: New approaches to the delivery of biopharmaceuticals. Trends in Pharmacological Sciences, 25(7), 382–387. doi:10.1016/j.tips.2004.05.006

Orr, G. a, Verdier-Pinard, P., McDaid, H., & Horwitz, S. B. (2003). Mechanisms of Taxol resistance related to microtubules. Oncogene, 22(47), 7280–7295. doi:10.1038/sj.onc.1206934

Papahadjopoulos, D., Allen, T. M., Gabizon, A, Mayhew, E., Matthay, K., Huang, S. K., Redemann, C. (1991). Sterically stabilized liposomes: improvements in pharmacokinetics and antitumor therapeutic efficacy. Proceedings of the National Academy of Sciences of the United States of America, 88(24), 11460–11464. doi:10.1073/pnas.88.24.11460

Parhi, P., Mohanty, C., & Sahoo, S. K. (2012). Nanotechnology-based combinational drug delivery: An emerging approach for cancer therapy. Drug Discovery Today, 17(17-18), 1044–1052. doi:10.1016/j.drudis.2012.05.010

Park, J., Fong, P. M., Lu, J., Russell, K. S., Booth, C. J., Saltzman, W. M., & Fahmy, T. M. (2009). PEGylated PLGA nanoparticles for the improved delivery of doxorubicin. Nanomedicine: Nanotechnology, Biology, and Medicine, 5(4), 410–418. doi:10.1016/j.nano.2009.02.002

Park, K. (2014). Controlled drug delivery systems: Past forward and future back. Journal of Controlled Release : Official Journal of the Controlled Release Society, 190, 3–8. doi:10.1016/j.jconrel.2014.03.054

Parveen, S., Misra, R., & Sahoo, S. K. (2012). Nanoparticles: A boon to drug delivery, therapeutics, diagnostics and imaging. Nanomedicine: Nanotechnology, Biology, and Medicine, 8(2), 147–166. doi:10.1016/j.nano.2011.05.016

Perrie, Y., & Rades, T. (2012). FASTtrack Pharmaceutics: Drug Delivery and Targeting (119-125). Pharmaceutical Press. Retrieved from https://books.google.com.tr/books?id=F9DNMYOG7IoC

Plapied, L., Duhem, N., des Rieux, A., & Préat, V. (2011). Fate of polymeric nanocarriers for oral drug delivery. Current Opinion in Colloid and Interface Science, 16(3), 228–237. doi:10.1016/j.cocis.2010.12.005

Pommier, Y., Leo, E., Zhang, H., & Marchand, C. (2010). DNA topoisomerases and their poisoning by anticancer and antibacterial drugs. Chemistry and Biology, 17(5), 421–433. doi:10.1016/j.chembiol.2010.04.012

Pouton, C. W., & Akhtar, S. (1996). Biosynthetic polyhydroxyalkanoates and their potential in drug delivery. Advanced Drug Delivery Reviews, 18(2), 133–162. doi:10.1016/0169-409X(95)00092-L

Pouton, C. W., Wagstaff, K. M., Roth, D. M., Moseley, G. W., & Jans, D. a. (2007). Targeted delivery to the nucleus. Advanced Drug Delivery Reviews, 59(8), 698–717. doi:10.1016/j.addr.2007.06.010

Prabaharan, M. (2015). Chitosan-based nanoparticles for tumor-targeted drug delivery. International Journal of Biological Macromolecules, 72, 1313–1322. doi:10.1016/j.ijbiomac.2014.10.052

Pradhan, M., Singh, D., & Singh, M. R. (2013). Novel colloidal carriers for psoriasis: Current issues, mechanistic insight and novel delivery approaches. Journal of Controlled Release, 170(3), 380–395. doi:10.1016/j.jconrel.2013.05.020

Probst, C. E., Zrazhevskiy, P., Bagalkot, V., & Gao, X. (2013). Quantum dots as a platform for nanoparticle drug delivery vehicle design. Advanced Drug Delivery Reviews, 65(5), 703–718. doi:10.1016/j.addr.2012.09.036

Prow, T. W., Grice, J. E., Lin, L. L., Faye, R., Butler, M., Becker, W., Roberts, M. S. (2011). Nanoparticles and microparticles for skin drug delivery. Advanced Drug Delivery Reviews, 63(6), 470–491. doi:10.1016/j.addr.2011.01.012

Safari, J., & Zarnegar, Z. (2014). Advanced drug delivery systems: Nanotechnology of health design A review. Journal of Saudi Chemical Society, 18(2), 85–99. doi:10.1016/j.jscs.2012.12.009

Safinya, C. R., & Ewert, K. K. (2012). Materials chemistry: Liposomes derived from molecular vases. Nature, 489(7416), 372–374. doi:10.1038/489372b

Sessa, G., & Weissmann, G. (1968). Phospholipid spherules (liposomes) as a model for biological membranes. Journal of Lipid Research, 9(3), 310–318.

Siepmann, J., Siegel, R. A., & Rathbone, M. J. (2011). Fundamentals and Applications of Controlled Release Drug Delivery. Springer US. Retrieved from https://books.google.com.tr/books?id=9yKSJdK37aMC

Sosnik, A., Carcaboso, Á. M., Glisoni, R. J., Moretton, M. a., & Chiappetta, D. A. (2010). New old challenges in tuberculosis: Potentially effective nanotechnologies in drug delivery. Advanced Drug Delivery Reviews, 62(4-5), 547–559. doi:10.1016/j.addr.2009.11.023

Steichen, S. D., Caldorera-Moore, M., & Peppas, N. a. (2013). A review of current nanoparticle and targeting moieties for the delivery of cancer therapeutics. European Journal of Pharmaceutical Sciences, 48(3), 416–427. doi:10.1016/j.ejps.2012.12.006

Sui, M., Liu, W., & Shen, Y. (2011). Nuclear drug delivery for cancer chemotherapy. Journal of Controlled Release, 155(2), 227–236. doi:10.1016/j.jconrel.2011.07.041

Swift, L. P., Rephaeli, A., Nudelman, A., Phillips, D. R., & Cutts, S. M. (2006). Doxorubicin-DNA adducts induce a non-topoisomerase II-mediated form of cell death. Cancer Research, 66(9), 4863–4871. doi:10.1158/0008-5472.CAN-05-3410

Szoka, F., & Papahadjopoulos, D. (1978). Procedure for preparation of liposomes with large internal aqueous space and high capture by reverse-phase evaporation. Proceedings of the National Academy of Sciences of the United States of America, 75(9), 4194–4198. doi:10.1073/pnas.75.9.4194

Tacar, O., Sriamornsak, P., & Dass, C. R. (2013). Doxorubicin: An update on anticancer molecular action, toxicity and novel drug delivery systems. Journal of Pharmacy and Pharmacology, 65, 157–170. doi:10.1111/j.2042-7158.2012.01567.x

Tewes, F., Munnier, E., Antoon, B., Ngaboni Okassa, L., Cohen-Jonathan, S., Marchais, H., Chourpa, I. (2007). Comparative study of doxorubicin-loaded poly(lactide-co-glycolide) nanoparticles prepared by single and double emulsion methods. European Journal of Pharmaceutics and Biopharmaceutics, 66(3), 488–492. doi:10.1016/j.ejpb.2007.02.016

Tkachenko, A. G., Xie, H., Liu, Y., Coleman, D., Ryan, J., Glomm, W. R., Feldheim, D. L. (2004). Cellular trajectories of peptide-modified gold particle complexes: Comparison of nuclear localization signals and peptide transduction domains. Bioconjugate Chemistry, 15(3), 482–490. doi:10.1021/bc034189q

Tsung, J., & Burgess, D. J. (2012). Fundamentals and Applications of Controlled Release Drug Delivery. Fundamentals and Applications of Controlled Release Drug Delivery, 107–23. doi:10.1007/978-1-4614-0881-9_5

Uchechi, O., Ogbonna, J. D. N., & Attama, A. (2014). Nanoparticles for Dermal and Transdermal Drug Delivery. Application of Nanotechnology in Drug Delivery 193–235. doi: 10.5772/58672

Urtuvia, V., Villegas, P., González, M., & Seeger, M. (2014). Bacterial production of the biodegradable plastics polyhydroxyalkanoates. International Journal of Biological Macromolecules, 70, 208–213. doi:10.1016/j.ijbiomac.2014.06.001

Vilar, G., Tulla-Puche, J., & Albericio, F. (2012). Polymers and drug delivery systems. Curr. Drug Deliv., 9(4), 367–394. http://doi.org/10.1146/annurev-chembioeng-073009-100847

Wagstaff, K. M., & Jans, D. a. (2009). Nuclear drug delivery to target tumour cells. European Journal of Pharmacology, 625(1-3), 174–80. doi:10.1016/j.ejphar.2009.06.069

Wang, A. Z., Langer, R., & Farokhzad, O. C. (2012). Nanoparticle Delivery of Cancer Drugs. Annual Review of Medicine, 63(1), 185–198. doi:10.1146/annurev-med-040210-162544

Wang, S., Konorev, E., Kotamraju, S., Joseph, J., Kalivendi, S., & Kalyanaraman, B. (2004). Doxorubicin induces apoptosis in normal and tumor cells via distinctly different mechanisms: Intermediacy of H2O2- and p53-dependent pathways. Journal of Biological Chemistry, 279(24), 25535–25543. doi:10.1074/jbc.M400944200

Wise, D. L. (2000). Handbook of Pharmaceutical Controlled Release Technology. Taylor & Francis. Retrieved from https://books.google.com.tr/books?id=paEzHRHlXE4C

Wong, B. S., Yoong, S. L., Jagusiak, A., Panczyk, T., Ho, H. K., Ang, W. H., & Pastorin, G. (2013). Carbon nanotubes for delivery of small molecule drugs. Advanced Drug Delivery Reviews, 65(15), 1964–2015. doi:10.1016/j.addr.2013.08.005

Xu, Z. P., Zeng, Q. H., Lu, G. Q., & Yu, A. B. (2006). Inorganic nanoparticles as carriers for efficient cellular delivery. Chemical Engineering Science, 61(3), 1027–1040. doi:10.1016/j.ces.2005.06.019

Yang, C., Wang, X., Yao, X., Zhang, Y., Wu, W., & Jiang, X. (2015). Hyaluronic acid nanogels with enzyme-sensitive cross-linking group for drug delivery. Journal of Controlled Release, 205, 206–217. doi:10.1016/j.jconrel.2015.02.008

Yang, F., Jin, C., Jiang, Y., Li, J., Di, Y., Ni, Q., & Fu, D. (2011). Liposome based delivery systems in pancreatic cancer treatment: From bench to bedside. Cancer Treatment Reviews, 37(8), 633–642. doi:10.1016/j.ctrv.2011.01.006

Yang, F., Teves, S. S., Kemp, C. J., & Henikoff, S. (2014). Doxorubicin, DNA torsion, and chromatin dynamics. Biochimica et Biophysica Acta - Reviews on Cancer, 1845(1), 84–89. doi:10.1016/j.bbcan.2013.12.002

Yilgor, P., Tuzlakoglu, K., Reis, R. L., Hasirci, N., & Hasirci, V. (2009). Incorporation of a sequential BMP-2/BMP-7 delivery system into chitosan-based scaffolds for bone tissue engineering. Biomaterials, 30(21), 3551–3559. doi:10.1016/j.biomaterials.2009.03.024

Zhang, H., Huang, S., Yang, X., & Zhai, G. (2014). Current research on hyaluronic acid-drug bioconjugates. European Journal of Medicinal Chemistry, 86, 310–317. doi:10.1016/j.ejmech.2014.08.067

Zhang, K., Tang, X., Zhang, J., Lu, W., Lin, X., Zhang, Y., He, H. (2014). PEG-PLGA copolymers: Their structure and structure-influenced drug delivery applications. Journal of Controlled Release, 183(1), 77–86. doi:10.1016/j.jconrel.2014.03.026

Zuber, M., Zia, F., Zia, K. M., Tabasum, S., Salman, M., & Sultan, N. (2015). Collagen based polyurethanes—A review of recent advances and perspective.

International Journal of Biological Macromolecules, 80, 366–374. doi:10.1016/j.ijbiomac.2015.07.001

APPENDIX A

DOXORUBICIN CALIBRATION CURVE

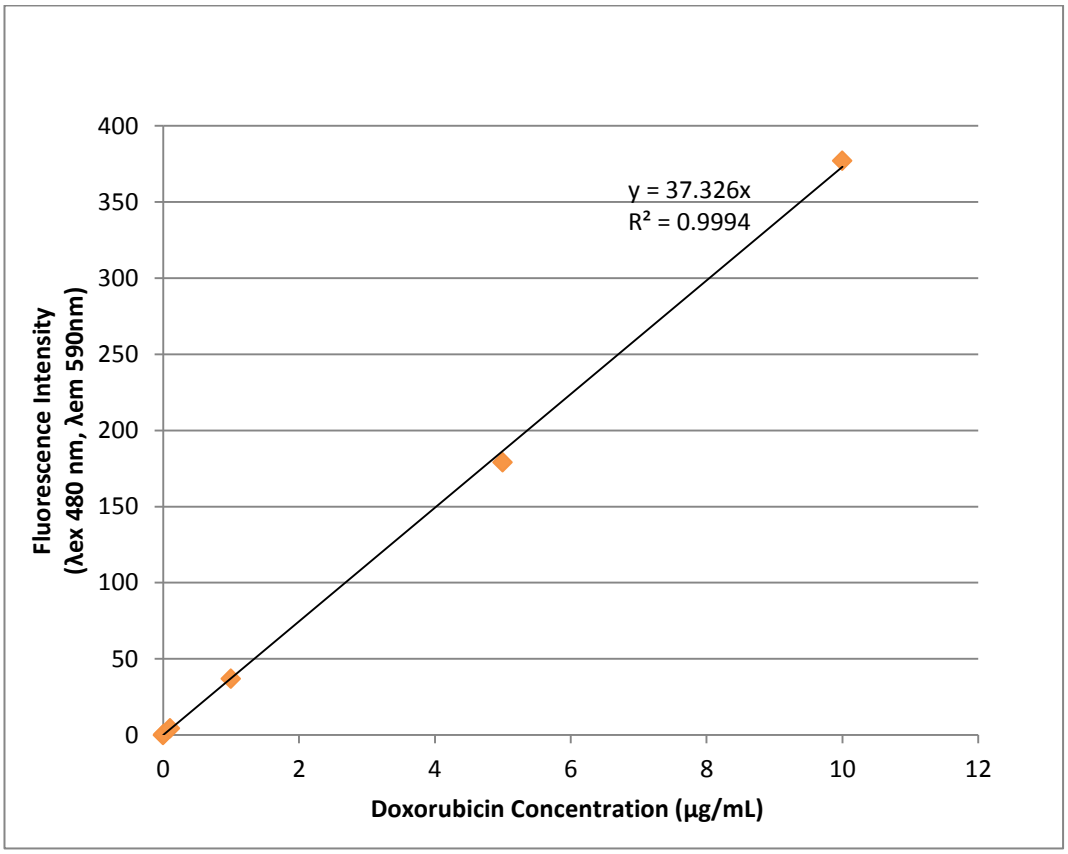

Figure 35: Calibration curve of Doxorubicin.

APPENDIX B

CALCEIN CALIBRATION CURVE

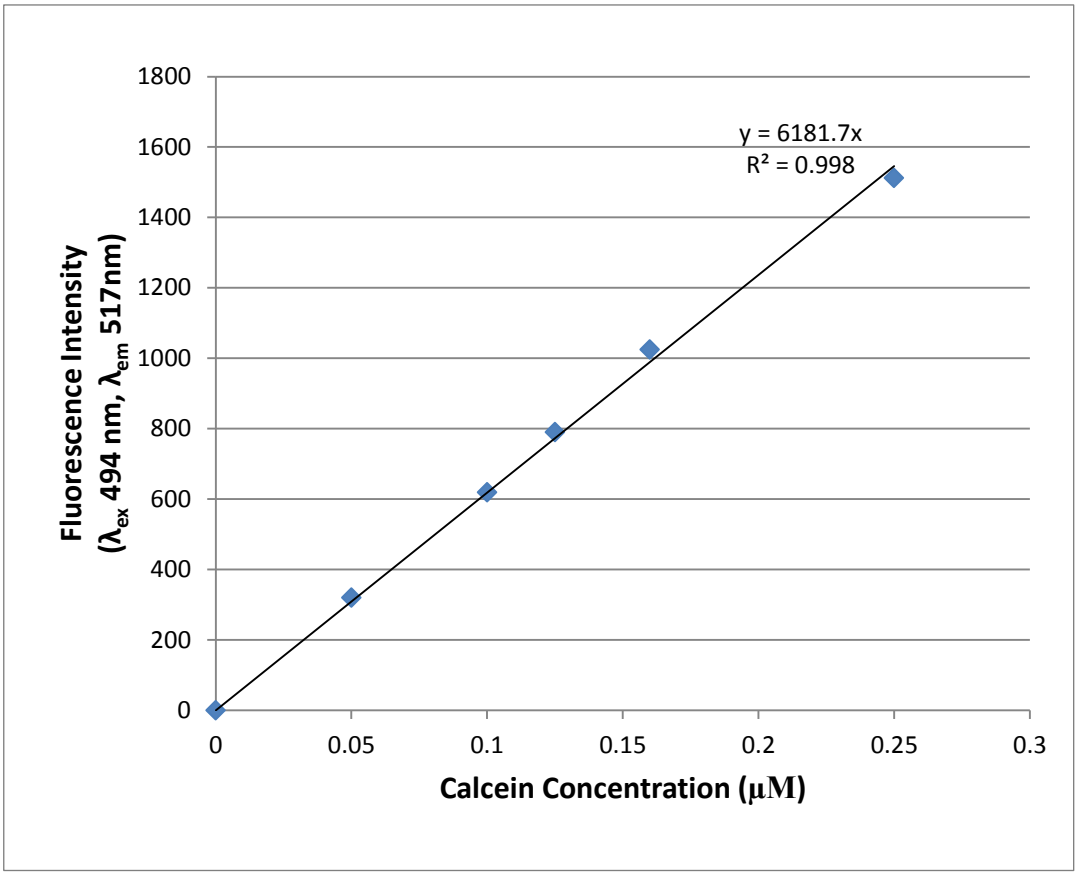

Figure 36: Calibration curve of Calcein.

APPENDIX C

THE PRINCIPLE OF ALAMAR BLUE ASSAY

Alamar Blue cell viability reagent monitors the cell viability by indicating the reduction power of the living cells where Resazurin, which is the active ingredient of Alamar Blue solution, is reduced to Resorufin by entering viable cells so that the color of the media surrounding the cells can be measured by reading the increase in the overall fluorescence. The color changes from blue to purple as a result of the reduction. The absorbance of the solution is measured at 570 nm (λ_1) and 595 nm (λ_2).

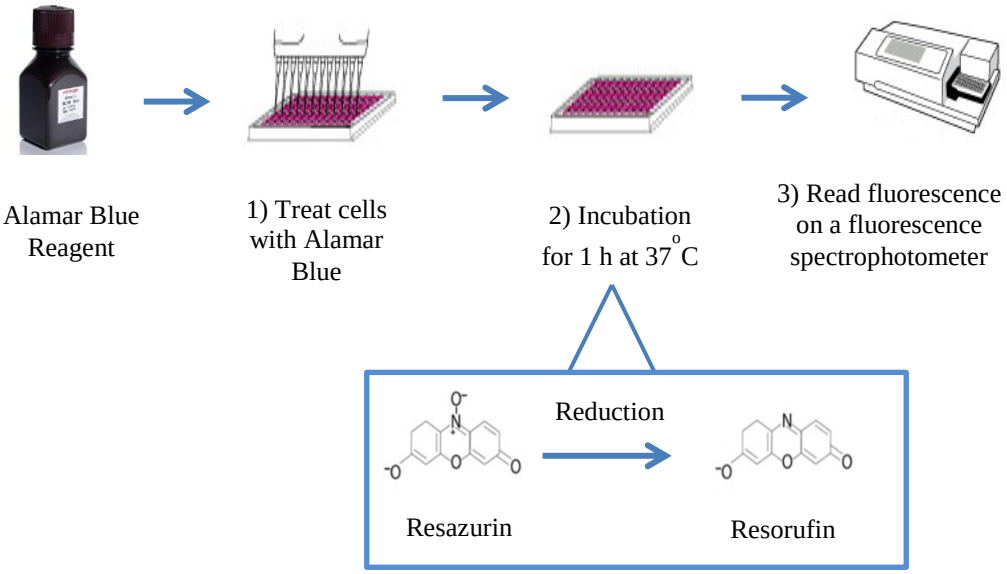

APPENDIX D

ALAMAR BLUE CALIBRATION CURVE FOR SAOS-2 CELLS (n=3)

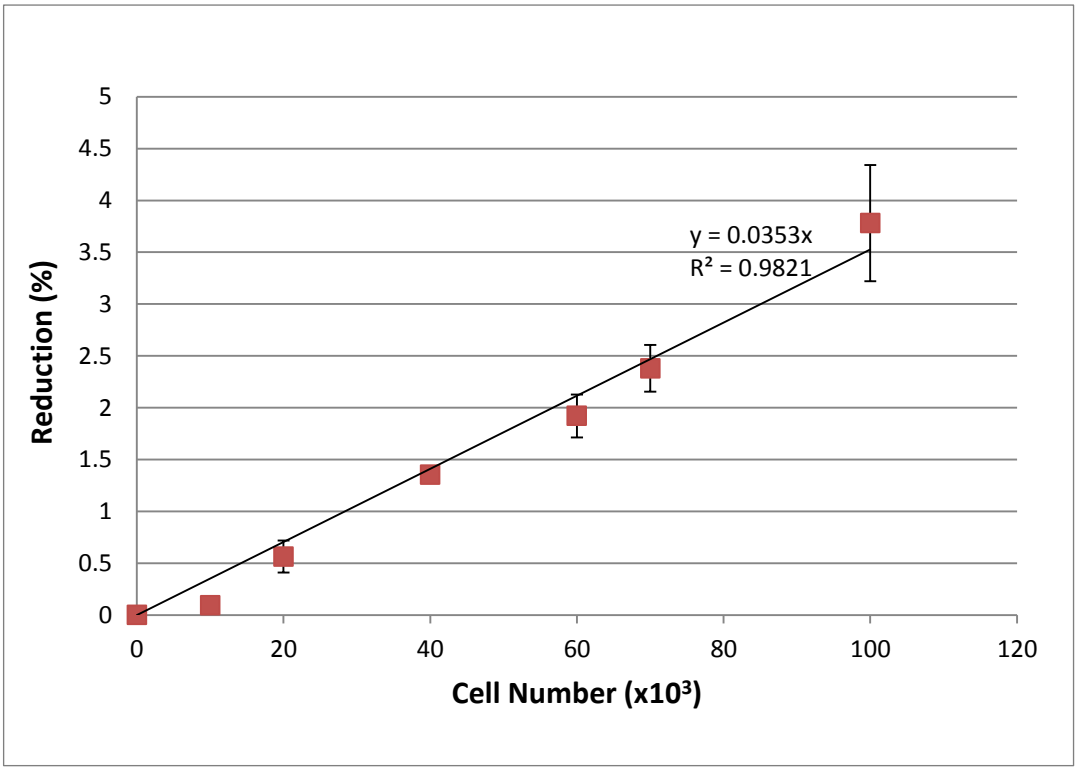

Figure 37: Alamar Blue calibration curve of Saos-2 cells.

APPENDIX E

THE MECHANISM OF EDC/ NHS CROSSLINKING

EDC (1-Ethyl-3-(3-dimethylaminopropyl)-carbodiimide)/ N-Hydroxysuccinimide (NHS) cross linking provides the only method for the labeling or crosslinking to carboxyl groups of peptides or proteins. For instance this carboxyl group may belong to C-terminus and side chains of glutamic acid and aspartic acid. To be able to accomplish this crosslinking, one must supply a large molar excess of the desired amine-containing molecule.

Step 1: EDC molecule reacts with carboxylic acid group of the substrate molecule:

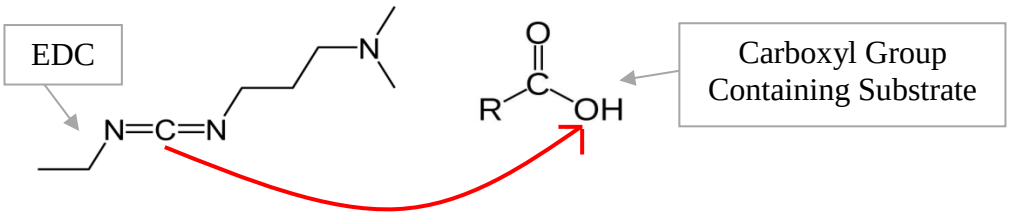

Step 2: EDC that reacts with carboxylic group forms an intermediate structure that is easily displaced by nucleophilic attack from primary amino groups in the reaction mixture. Thus, this intermediate structure reacts with NHS molecule:

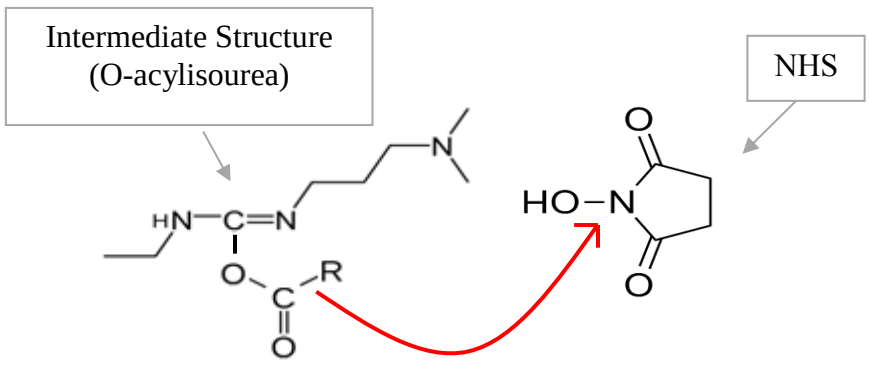

Step 3: EDC finally coupled NHS to carboxyls, forming an NHS ester that is considerably more stable than the O-acylisourea intermediate, so EDC allows for efficient conjugation to primary amines at physiological pH:

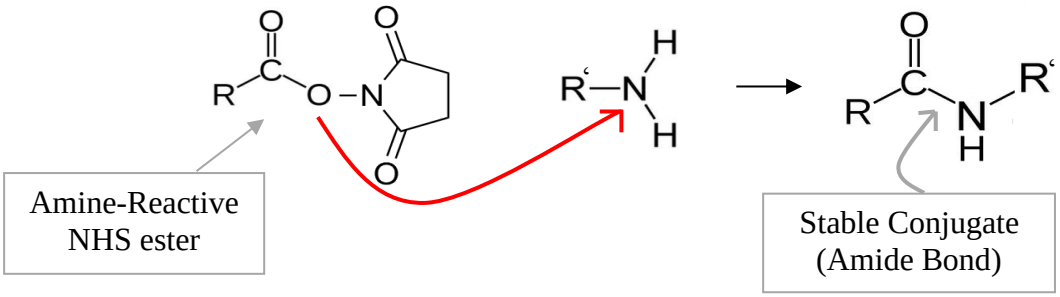

R= PHBV, R‘= NLS